

Powering Mining Sites with Renewables: Comparative Economic and Environmental Analysis across Sites Worldwide

MASTER THESIS

LAZAR TOMANI



Universiteit Leiden



Powering Mining Sites with Renewables: Comparative Economic and Environmental Analysis across Sites Worldwide

Master Thesis Report

Industrial Ecology

Leiden University (**65003**) x TU Delft (**6117317**)

Author

Lazar Tomani

Supervisors

Dr. I.R. Istrate

Dr. E. (Enno) Schröder

19/09/2025

Abstract

Lithium is a significant material of the energy transition, powering electric vehicles and grid storage, and surging demand is expanding extraction, yet lithium mining is energy intensive and can impose significant environmental burdens. This thesis evaluates whether on-site renewables plus battery energy storage systems (BESS) can provide reliable, cost-competitive, lower-carbon electricity for 39 lithium mines across 10 countries. I compare solar, wind, and hybrid systems paired with either about 3 hours (near autonomous) or about 12 hours (fully autonomous) of storage. The calculated levelized cost of electricity (LCOE) spans from USD 0.07 to 0.17 per kWh, consistently below diesel generation costs (0.24–0.38 \$/kWh) and broadly competitive with grid tariffs (0.06–0.15 \$/kWh) across the countries studied. Internal rates of return (IRR) range from –4 percent to +48 percent, and paybacks from 0.4 to 10 years under a 20-year baseline life. Life-cycle assessment indicates more than 90 percent CO₂ reductions versus diesel or carbon-intensive grids. A clear autonomy-versus-cost trade-off emerges: moving from about 98 percent renewable power supply with 3 hours of storage to 100 percent supply with 12 hours raises capital intensity, lifting LCOE and lowering IRR and net present value (NPV), while adding only modest extra emissions abatement. Technology choice is second order but directional: where wind resources are strong it tends to deliver the lowest LCOE and highest returns, while hybrids reduce resource mismatch risk and often beat baseline tariffs. Sensitivity and robustness tests show IRR and NPV are driven mainly by avoided-cost factors such as diesel and grid prices, and economics weaken at grid-supplied sites and in short-life mines of 10 to 5 years. Beyond economics, the study shows that all-renewable systems reduce emissions but shift the environmental burden onto land and raw materials. Photovoltaic (PV) systems occupy more land than wind, while longer storage multiplies demand for critical raw materials and adds pressure to their supply chains. Overall, renewable energy systems with BESS can decarbonize lithium extraction at competitive cost where resources and lifetimes are favourable and conventional energy is expensive, though they also introduce new land and material pressures that must be managed.

Contents

| | |
|--|----|
| Abstract | 1 |
| Abbreviations..... | 4 |
| 1. Introduction | 6 |
| 2. Literature review | 7 |
| 3. Methods | 10 |
| 3.1 Overview of methodology | 10 |
| 3.2 Renewable system design..... | 11 |
| 3.2.1 Scenario design | 11 |
| 3.2.2 Baseline Annual Electricity Demand and Renewable Energy Generation | 12 |
| 3.3 Techno-economic analysis | 14 |
| 3.3.1 Key metrics | 17 |
| 3.4 Environmental assessment | 18 |
| 3.4.1 Material requirement | 18 |
| 3.4.2 Land-use..... | 18 |
| 3.4.3 Lifecycle GHG emissions | 19 |
| 3.5. Sensitivity analysis | 19 |
| 3.5.1 Key parameters sensitivity | 19 |
| 3.5.2 Energy-Source Sensitivity Analysis..... | 20 |
| 3.5.3 Mine-Life Sensitivity | 21 |
| 3.5.4 Optimized hybrid renewable system..... | 21 |
| 3.6 Assumptions and Limitations | 22 |
| 4. Results..... | 23 |
| 4.1 Technoeconomic results..... | 23 |
| 4.1.1 System scale and feasibility | 24 |
| 4.2 Technoeconomic key metrics across scenarios | 25 |
| 4.2.1 Effects of storage duration | 25 |
| 4.2.2 Effects of technology..... | 26 |
| 4.3 Technoeconomic findings by country | 29 |
| 4.3.1 Levelized cost of energy and scale effects by country | 29 |
| 4.3.2 Payback period by country | 30 |
| 4.3.3 Net present value by country..... | 31 |
| 4.3.4 Internal rate of return by country | 31 |

| | |
|---|----|
| 4.4 Environmental impact | 32 |
| 4.4.1 Land use | 32 |
| 4.4.2 Material consumption | 34 |
| 4.4.3 Greenhouse gas emissions | 35 |
| 4.5 Sensitivity analysis | 37 |
| 4.5.1 Robustness of financial performance under parameter variation | 37 |
| 4.5.2 Energy-supply assumption robustness | 40 |
| 4.5.3 Mining sites lifespan assumption robustness | 41 |
| 4.5.4 Effects of hybrid renewable system optimization on technoeconomic results | 42 |
| 5. Discussion | 43 |
| 5.1 Interpretation of key findings | 43 |
| 5.2 Comparison with literature | 44 |
| 6. Conclusion | 45 |
| Acknowledgments | 46 |
| References | 47 |
| Appendices | 52 |

Abbreviations

BESS Battery Energy Storage System(s)

BOS Balance of System

CAPEX Capital Expenditure

CO₂ Carbon Dioxide

CO₂eq Carbon Dioxide Equivalent

CRF Capital Recovery Factor

CRM Critical Raw Materials

CSP Concentrating Solar Power

DCF Discounted Cash Flow

DoD Depth of Discharge

EEA European Environment Agency

EPA U.S. Environmental Protection Agency

GHG Greenhouse Gas(es)

GWh Gigawatt-hour(s)

HOMER (Pro) Hybrid Optimization of Multiple Energy Resources (software)

HRES Hybrid Renewable Energy System

IEA International Energy Agency

IRENA International Renewable Energy Agency

IQR Interquartile Range

IRR Internal Rate of Return

kW Kilowatt

kWh Kilowatt-hour

Li-ion Lithium-ion (battery)

LCE Lithium Carbonate Equivalent

LCOE Levelized Cost of Energy (or Electricity)

LHV Lower Heating Value

MW Megawatt

MWh Megawatt-hour(s)

NREL National Renewable Energy Laboratory

NCF Net Cash Flow

NEA Nuclear Energy Agency

NPV Net Present Value

NPC Net Present Cost

O&M Operations & Maintenance

OECD Organisation for Economic Co-operation and Development

PBT Payback Period

PV Photovoltaic

PVPS (IEA-PVPS) Photovoltaic Power Systems Programme

R^2 Coefficient of Determination

RTE Round-Trip Efficiency

TAC Total Annualized Cost

TEA Techno-Economic Analysis

WACC Weighted Average Cost of Capital

USD United States dollar

t tonne (metric ton)

kt kilotonne

GW Gigawatt

1. Introduction

Mining operations are responsible for a substantial share of global greenhouse gas (GHG) emissions, contributing 4–7 % of the worldwide total (Aramendia et al., 2023). Most operations rely on diesel generators or carbon-intensive electricity grids, leading to high operating costs and significant emissions (Aramendia et al., 2023; Ataei & Barabadi, 2023). Cutting this reliance on fossil energy will require new approaches, and one promising way is to incorporate more renewable energy directly into mining operations. Several studies demonstrate that renewable energy systems can supply reliable power to mines while improving sustainability indicators (Aramendia et al., 2023; Pouresmaeli et al., 2023). These carbon free technologies themselves depend on raw materials supplied by mining, and as a result, it is essential that the mining sector be decarbonized to avoid undermining their overall positive environmental impact of renewable energy (Li et al., 2024; Zharan & Bongaerts, 2017; Dellicompagni et al., 2021).

Certain raw material stand out as strategic priorities for carbon free energy technologies. Among them, lithium is of particular interest serving as a key material for lithium-ion batteries that power electric vehicles and support grid-scale renewable energy storage (Li et al., 2024). As global economies electrify transport systems and expand renewable deployment, the demand for lithium is expected to rise rapidly in the coming decades (Huang et al., 2024; Li et al., 2024). However, lithium extraction remains energy and carbon intensive, leaving operators vulnerable to volatile fuel prices and undermining the climate benefits of the technologies that depend on lithium (Mertens et al., 2024; Aramendia et al., 2023).

In this thesis, lithium mining is used as a representative case study to explore the wider potential for renewable energy integration across the mining sector. Lithium sites offer a relevant test case due to their strategic importance in the energy transition and diverse geographical distribution.

To that end, I analyse lithium mines worldwide using a consistent dataset of electricity expenditure records. At each site, I apply the same input values and sizing rules to six predefined renewable power systems alongside with battery storage (solar, wind, and a 50:50 hybrid, each with 3 h or 12 h of storage) and compare their performance across geographies and operating contexts. The sample includes all lithium sites for which the available data support a credible techno-economic and environmental assessment, although it does not cover every mine globally. The overarching objective is to evaluate the techno-economic feasibility and environmental trade offs of renewable-plus-storage systems in mining. The study main research questions is *what is the techno-economic*

and environmental performance of on-site renewable-energy systems with storage across lithium mining sites in different regions and operating conditions? and aims to address three sub-questions:

- RQ1: How do techno-economic indicators performance vary across different scenarios and lithium mining sites?
- RQ2: . How do material requirements, land footprint, and life-cycle GHG emissions of renewable integration in mines vary across different scenarios and lithium mining sites?
- RQ3: How sensitive are the results to changes in key assumptions, and which factors primarily drive the differences?

2. Literature review

In the last decade, solar photovoltaic, wind, and battery energy storage system technologies have seen drastic cost reductions, encouraging trials of these technologies at mining sites (Maennling & Toledano, 2018). Many of the mining sites still have diesel generators as backup for reliability, even if the use of renewable energy is growing (Paneri et al., 2021). In one example, a mine in Australia still uses 19 MW of diesel generators while having a 10.6 MW solar PV array and 6 MW of battery storage (Ellabban & Alassi, 2021). Researchers frequently incorporate conventional energy sources into their simulated studies, due to their role as a backup for resilience or peak demand (Ranjbar et al., 2024; Paneri et al., 2021).

Many works in this area rely on simulation-based approaches to evaluate how renewable energy systems might perform in mining environments. One such example is the study by Bitaraf and Buchholz (2018), who modelled four off-grid scenarios using the software HOMER Pro for energy system optimization. The four scenarios considered were a diesel-only baseline, diesel combined with battery storage, diesel with solar PV, and a hybrid configuration combining diesel, PV, and batteries (Bitaraf & Buchholz, 2018). Their findings indicated that adding solar and battery storage significantly cut fuel use and resulted in lower energy costs per kWh compared to other setups (Bitaraf & Buchholz, 2018). The most influential economic factors of those results were the diesel price and upfront cost of PV (Bitaraf & Buchholz, 2018). However, this study was limited to a single site and tested only one battery configuration without exploring the impact of varying renewables

potential across geographical locations, different storage durations, or the feasibility of 100% renewable electricity production (Bitaraf & Buchholz, 2018).

Maronga et al. (2021) model renewable system integration into a grid-connected mine in Zimbabwe (platinum, palladium, rhodium, gold, nickel, copper), testing photovoltaics with battery storage and sweeping storage from 2–12 h. The cost-optimal setup supplies approximately 63% of annual demand, with the grid covering the rest (Maronga et al., 2021). The study does not target near or full renewable electricity supply, remains single-site with no cross-site comparison, and does not assess off-grid reliability at high renewable penetration (Maronga et al., 2021).

Ellabban and Alassi (2021) used also HOMER Pro to model optimal hybrid system sizing for three Australian mining sites, including a real-world replication a copper and gold mine. Over six years, the project reached a renewable penetration of 17%, below the original 21% target. Their analysis showed that integrating solar PV and battery storage led to annual reductions of 5 million litres of diesel and 12,000 tonnes of carbon emissions (Ellabban & Alassi, 2021). While this real-world case supports the potential of hybrid renewable systems, it also highlights that full renewable autonomy remains hard to reach because they are still heavily influenced by site-specific factors like solar irradiance and load consistency (Ellabban & Alassi, 2021).

In the South Africa, Nkambule et al. (2023) evaluated a hybrid energy setup integrating floating PV, wind turbines, and vanadium redox flow batteries. The system showed promising financial outcomes, achieving an internal rate of return of 23.5%, which reflects the profitability of the investment relative to its cost over time (Nkambule et al., 2023). The reported payback period was 4.9 years, showing how long it would take to recover the initial financial investment (Nkambule et al., 2023). In terms of cost efficiency, the levelized cost of electricity, a metric that spreads the total system costs across its operational lifetime, was estimated at roughly 0.23 USD per kilowatt-hour, positioning the system as economically competitive (Nkambule et al., 2023). From an environmental standpoint, the hybrid configuration cut annual CO₂eq emissions by roughly 1.74 million kilograms (Nkambule et al., 2023). The study scope is confined to a single mine and does not assess transferability to other commodities, such as lithium, or to geographically diverse operations (Nkambule et al., 2023).

One study available exploring lithium-specific operations is by Dellicompagni et al. (2021), who simulate the integration of concentrating solar power into lithium mining operations in Argentina. Their analysis suggests that using a parabolic trough concentrated solar power plant with thermal storage could cover more than half of the mine's energy needs and cut emissions by over 400 grams of CO₂ per kilogram of lithium carbonate equivalent produced. While these findings shows the

technical and environmental potential of concentrated solar power in remote lithium mining regions, the study lacks a techno-economic assessment. As noted by Li et al. (2024), who reference this work in their review, such modelling attempts remain rare. Despite lithium's central role in the global energy transition, dedicated economic and performance modeling for renewable-powered lithium mining remains heavily underrepresented in the academic literature (Dellicompagni et al., 2021; Li et al., 2024).

On environmental impacts, most peer-reviewed studies focus narrowly on CO₂ emissions from renewable integration in mining. At the Fekola Gold Mine in Mali, for instance, a 30 MW solar PV array with 17 MWh of battery storage preventing approximately 39,000 tonnes of CO₂ emissions annually and saving 13 million litres of fuel (Issa et al., 2023). According to Dellicompagni et al. (2021), modelling in lithium brine mining with CSP and thermal storage achieved over 50% renewable electricity share, which translates to 403.3 g CO₂ saved per kilogramme of lithium produced. Despite these encouraging results, wider environmental trade-offs such as the land transformation and material footprint associated with manufacturing and operating the renewable power system remain largely unaddressed in most studies (Issa et al., 2023; Li et al., 2024; Dellicompagni et al., 2021).

While much of the existing research is site-specific, Li et al. (2024) provide a broad overview of international RE projects in mining but do not conduct a harmonised techno-economic comparison across countries. This is where my thesis steps in, using a consistent global framework. A further gap in the literature is the lack of detailed techno-economic analysis comparing longer battery storage durations with partial diesel backup. While one mine study does sweep battery storage duration for PV plus batteries (Maronga et al., 2021), it is grid-connected and reaches only ~63% annual renewable electricity supply, with the grid covering the remainder. My thesis examines this by evaluating 3-hour and 12-hour battery configurations to assess whether extended storage is required to achieve 100% reliability or if a 2% diesel backup offers a more cost-effective solution. Unlike previous studies that only model partial renewable electricity supply, my work examines systems designed to meet 100 % of annual mining electricity demand with renewables and at the same time compare different storage capacities.

In short, although the literature provides valuable examples of renewable energy deployment in mining, it is still narrow in scope, often restricted to one or two sites and largely confined to GHG metrics without considering other environmental burdens. My thesis aims to fill these gaps through a global comparative analysis of 39 lithium mining sites, applying standardised modelling assumptions across all cases. By comparing short- and long-duration BESS configurations and

applying a 1.5× overbuild factor, I provide a systematic assessment of fully renewable mining power systems, moving beyond isolated case studies to deliver cross-regional insights on economic feasibility and environmental trade offs.

3. Methods

In order to assess the economic viability and environmental impact of integrating renewable energy at mining sites, I calculate the required energy system capacity and evaluate economic and environmental indicators. I calculate each site's electricity demand from reported electricity expenditures and use this to size the renewable generation and battery-energy-storage system. After sizing the systems across all sites and scenarios, I compute the techno-economic metrics: net present value (NPV), internal rate of return (IRR), levelized cost of energy (LCOE), and the discounted payback period. These metrics assess economic feasibility and enable comparisons across sites and technologies. To evaluate environmental trade-offs, I quantify the material intensity and land-use of the sized renewable systems, and I assess life cycle CO_{2eq} emissions relative to the pre-transition baseline (diesel or grid) to report avoided emissions.

3.1 Overview of methodology

This section outlines the tools and methodology employed to conduct a techno-economic and environmental assessment of 39 lithium mines transitioning to run on fully renewable energy systems. By converting reported per-tonne electricity expenses, expressed in dollars spent on electricity per ton of Lithium carbonate equivalent (LCE) produced, I calculated the total site electricity consumption and sized the renewable generation and battery-storage capacities by applying the overbuild factors and storage-hour requirements outlined by Tong et al. (2021) to achieve 98 or 100% system reliability. For each mine I evaluate six distinct renewable configurations—wind-only, solar-only and a 50/50 wind-solar hybrid, each paired with either 3 h or 12 h of battery storage. The analysis therefore models an integrated energy system comprising photovoltaic arrays, wind turbines, battery-energy-storage systems, and (in the few cases where 100 % reliability cannot be met by renewables alone) diesel back up.

I test NPV per tonne LCE, LCOE, IRR, and the discounted payback period across all system configurations and sites. Those metrics allow to test economic feasibility and compare performance across scenarios (Samatar et al., 2025). A Python script was used to perform the techno-economic analysis by combining the site-level inputs and converting them into annual cash-flow streams. Those streams include capital expenditures, O&M costs, scheduled asset replacements, end-of-life and energy savings. I use the term “energy savings” on the positive cash flows that are not spent on buying conventional energy, in order to provide more insight into the financial benefits of transitioning to renewable energy. The annualize total costs is calculated and used to derive the levelized cost of energy in dollars per kilowatt-hour of electricity provided to the mining site. The main inputs for the technoeconomic assessment can be found in table 2.

3.2 Renewable system design

3.2.1 Scenario design

This study examines 39 lithium-extraction mining sites across ten countries, China, Australia, Argentina, Brazil, Chile, Canada, Mali, Portugal, Zimbabwe, and the United States, with annual outputs ranging from under 1 kt to over 200 kt of LCE. Annual energy demand about each site can be found in Table A1 (Appendix A).

To compare viable pathways for decarbonizing mine-site electricity, I evaluate six standardized renewable configurations formed by crossing two dimensions:

- Generation mix: solar-only (PV), wind-only (Wind), and a 50:50 PV–Wind hybrid
- Storage duration: 3 hours vs 12 hours of storage sized to the site’s mean load.

I use six standardised mixes: PV-only, wind-only, and a 50:50 PV–wind hybrid, each evaluated with 3 h and 12 h storage. As shown in the literature review, there are no studies in which a mine receives 100% of its electricity needs from renewables. I therefore set two reliability targets to test whether renewables can supply almost all site electricity. Tong et al. (2021) report results for optimized solar–wind systems, where the solar share typically ranges between about 15% and 45% when applying their 1.5× overbuild and storage approach. In their analysis, these optimized mixes deliver electricity with 98% reliability when paired with 3 h battery storage, while extending storage to 12 h

raises this further to around 99.9%, though some countries still experience rare multi-day shortages. Tong et al. (2021) do not report values for Portugal, Mali, or Zimbabwe; for comparability I assume the same pattern for these three countries. In my study, I apply Tong's reported reliability outcomes to three designs (solar-only, wind-only, and 50:50 hybrid) in order to explore techno-economic and environmental trade-offs across 39 lithium mine sites. This represents a simplification, since pure-solar or pure-wind systems would not typically reach the same reliability at equal overbuild and storage, so my results likely overstate the reliability of single-technology cases. Accordingly, the 3 h designs are treated as "near-renewable," supplying 98% of annual electricity with 2% diesel back-up, while the 12 h designs are assumed to achieve 100% renewable supply (no diesel). For the 3 h scenarios the 2% comes from diesel, and only the price of diesel is taken into account, leaving out equipment and maintenance costs. This framing allows me to quantify the incremental economic (LCOE, IRR, NPV per t LCE, payback) and environmental (CO₂, materials, land) effects of adding extra storage across different lithium sites and countries.

3.2.2 Baseline Annual Electricity Demand and Renewable Energy Generation

I obtained the data on annual lithium carbonate equivalent (LCE) output and electricity spend (USD/t LCE) for each mine from the S&P Capital IQ Pro platform database (S&P Global Market Intelligence, 2025). Because the only reported data are annual LCE output and electricity spend, I make a few assumptions to recover each site's annual electricity demand. First, I assign a benchmark electricity intensity (kWh/t LCE) by production route for each site. For brine sites, I use site-specific values where available and otherwise country-level values from Schenker and Pfister (2025), with 1,200 kWh/t applied as a fallback. For hard-rock sites, a value of 7,718.75 kWh/t is applied uniformly across all mines (author's calculation; see Appendix I).

I multiply this benchmark by the national grid tariff (USD/kWh) to obtain an expected grid cost per tonne and use it to classify the power source, either grid electricity or diesel generators. In the absence of data, I assume the energy source through a parity based imputation: if my calculated estimate (in which I use grid prices) is equal or smaller than the reported spend, the site is treated as it supplies electricity through grid, otherwise as it uses diesel. Because detailed fuel mixes are unavailable, I assume one primary source per site in this step (i.e., without combining grid with diesel generators). I test the impact of this assumption in the sensitivity analysis by forcing all sites use electricity produced by diesel generators or grid.

Once the primary electricity source is determined, the electricity intensity per tonne of LCE produced is calculated. For grid-classified sites, I derive electricity intensity (kWh/LCE) by dividing reported spend (\$/t) by the grid tariff (\$/kWh). For diesel-classified sites, I convert the pump price of diesel (USD/L) into an effective electricity price (USD/kWh) by dividing it by the fuel's lower-heating-value energy per litre and the generator's electrical efficiency (see Appendix K). Multiplying the resulting kWh/t by annual LCE output (t/y) gives each site's annual electricity demand (kWh/y).

Renewable generation is sized against this demand using an overbuild factor of 1.5× to reflect the variability of wind and solar and to target high reliability (Tong et al., 2021). Concretely, I convert annual demand to mean load (kW), apply the 1.5× overbuild to mean load, and divide by the applicable national or regional capacity factor is applied to obtain the installed capacity for each option, following Tong et al. (2021).

Following Tong et al. (2021), I bracket storage depth with two designs (3 h and 12 h) sized to the site's mean load. Because only part of a battery is usable and cycling incurs losses, I convert the target delivered energy to nameplate using 80% depth-of-discharge and 85% round-trip efficiency (Augustine & Blair, 2021). Battery lifetime can range from 7 to 15 years depending on site conditions and location; for this study, I assume a global average of 10 years (Smith, Shi, Wood, & Pesaran, 2017; International Renewable Energy Agency, 2017). I assume the mine's project life matches the renewable system life, both set to 20 years, consistent with common practice in mining-microgrid studies (Nkambule et al, 2023). All parameter values and their sources are summarized in Table 1.

Table 1 Key input parameters and assumptions for baseline electricity demand estimation and renewable system sizing

| Parameter | Unit | Value / Rule | Citation |
|---|-------|---|--|
| Benchmark electricity intensity (brine) | kWh/t | Site-specific where available; else country-level values; if unavailable, 1,200 kWh/t | Schenker & Pfister (2025) |
| Benchmark electricity intensity (hard rock) | kWh/t | 7,718.75 | Burgess (2012); Góralczyk et al. (2020); Dessemond et al. (2019) |

| | | | |
|--|--------------|--------------------------|--------------------------|
| Diesel density | kg/L | 0.846 | EEA (2024) |
| Diesel lower heating value (mass basis) | kWh/kg | 11.83 | EEA (2024) |
| Energy prices (grid, diesel) | \$/kWh; \$/L | Country-specific | GlobalPetrolPrices, 2025 |
| Capacity factors (PV, wind) | – | Country/region averages; | Tong et al. (2021) |
| Generator electrical efficiency (baseline) | – | 0.35 | U.S. EPA (2017) |

3.3 Techno-economic analysis

Building on Sokolov (2024) and adopting the TEA structure from Samatar et al. (2025), I evaluate each configuration using CAPEX, NPV, IRR, discounted payback, LCOE, and NPV per tonne of LCE. CAPEX is the sum over components of installed capacity multiplied by unit cost. I then construct the annual cash-flow series: CAPEX, O&M, scheduled replacements, and (for the 3 h cases) diesel backup on the cost side; avoided diesel/grid purchases as positive inflows (Miller et al., 2021; Brady et al., 2020). Definitions and practical interpretations of these metrics are summarized in Table 2.

Table 2 Definitions of techno-economic metrics

| Metric | Definition | What it means in practice | Source |
|---|---|--|---------------------------------------|
| Net present value (npv) | The discounted sum of all future cash inflows minus outflows over the project's life. A positive NPV indicates that the project generates more value than it costs. | If $NPV > 0$, the project increases wealth and is financially viable. | (Sokolov, 2024) |
| Internal rate of return (irr) | The discount rate that makes $NPV = 0$. It measures the project's effective rate of return. | In practice, IRR is compared against the required return (hurdle rate). If IRR exceeds this, the project is considered attractive. In this report the hurdle rate is 10%. | (Sokolov, 2024) |
| Payback period (pp) | The time required for cumulative cash inflows to equal the initial investment (can be simple or discounted). | Shows how quickly invested capital is recovered. A payback of 3 years means the project "breaks even" in 3 years. Often preferred in risky contexts where early recovery is valuable. | (Sokolov, 2024; Samatar et al., 2025) |
| Levelized cost of electricity (lcoe) | The average lifetime cost per unit of electricity generated, including capital, O&M, fuel, and replacements. | Enables comparison across technologies. Example: $LCOE = \$0.05/kWh \rightarrow$ every kWh costs 5 cents over the system's life. A project is competitive if its LCOE is below grid/diesel prices. | (Samatar et al., 2025) |

The IRR is the rate that sets NPV = 0 (Sokolov, 2024). I define NPC as the present value of cost-only cash flows (CAPEX, O&M, replacements, backup in 3 h cases), explicitly excluding savings, consistent with Samatar et al. (2025). The discounted payback period is the first year in which cumulative discounted net cash flow becomes non-negative (Sokolov, 2024). Finally, I report NPV per tonne of LCE to normalize across different site sizes.

I assume a 20-year project life, with sensitivity analyses at 10 and 5 years. A real discount rate of 5% is applied to OECD sites and 7.5% to non-OECD sites. The analysis is pre-tax, excluding inflation, subsidies, carbon pricing, owner's costs. All capital expenditure (CAPEX) is incurred at t=0, while operating and other cash flows are accounted for at the end of each year. In the 3 h storage cases, the 2% diesel backup share is costed as fuel only, assuming existing standby gensets without additional CAPEX or O&M. No export revenues are considered, as systems are modeled as off-grid self-supply. Component replacements follow stated lifetimes (e.g., BESS at 10 years). Constant annual delivered electricity is assumed between replacements, with no explicit performance degradation modelled. Key input values used for these calculations are shown in Table 3.

Table 3 Base input values for techno-economic analysis

| Input | Base value | Citation |
|---------------------------------|-------------------|-----------------------|
| | | IRENA (2022) |
| PV CAPEX | \$758/kW | IRENA (2022) |
| PV O&M rate | 1.5% of CAPEX/yr | IRENA (2022) |
| Wind CAPEX | \$1,160/kW | IRENA (2022) |
| Wind O&M rate | 3% of CAPEX/yr | IRENA (2022) |
| Battery CAPEX | \$273/kWh | IRENA (2022) |
| Battery O&M rate | 0.43% of CAPEX/yr | Mongird et al. (2020) |
| Discount rate (OECD) | 5% real | IRENA (2022) |
| Discount rate (non-OECD) | 7.5% real | IRENA (2022) |

3.3.1 Key metrics

1) Net Present Value

The Net Present Value represents the total lifetime net benefit of the system in today's dollars by discounting each year's net cash flow back to time zero:

$$NPV = \sum_{t=0}^N \frac{CF_t}{(1 + R)^t}$$

- $CF_0 = -CAPEX$, is the negative up-front investment cost, entered as a negative value to reflect the outflow in year 0.
- $CF_t = E_t - O\&M_t - R_t - B_t$ ($t = 1, \dots, N - 1$),
- $CF_N = E_N - O\&M_N - R_N - B_N + S$
- R is the real discount rate; N is the project life (years); E_t is the energy-cost savings in year t ; R_t is the replacement cost in year t ; B_t is the backup energy cost in year t ; and S is the net salvage value at year N (positive if a benefit, negative if a decommissioning cost). A positive NPV means the discounted inflows exceed the discounted outflows at the rate R .

2) Total Annualized Cost

Having isolated all purely cost-side cash flows (CAPEX, O&M, replacements, backup, salvage) into a NPC, the TAC is simply that NPC annualized via the CRF:

$$TAC = NPC \times CRF$$

This spreads capital expenditure, O&M, replacements, backup, salvage value, etc., evenly over each year.

3) Levelized Cost of Electricity

The LCOE expresses the average cost per unit of electricity over the system's life by dividing the TAC by the yearly discounted energy output E_y :

$$\text{LCOE} = \frac{\text{TAC}}{\text{E}_y}$$

E_y is the annual delivered electricity. The LCOE thus indicates how much each Kwh “costs” when both capital and operating expenses are spread evenly across actual production.

3.4 Environmental assessment

In this study, I evaluate three key environmental impact indicators. Total material requirement, land-use, and lifecycle GHG emissions (expressed as CO₂-eq) are calculated by scaling well-established, per-unit benchmarks to each system’s installed capacity (see Appendix E for the benchmark values and Appendix F for their source references).

3.4.1 Material requirement

I derive the critical materials (aluminium, copper, graphite, silver, neodymium, dysprosium, lithium) contained in each energy system by multiplying a published material intensity (kilograms per kilowatt-hour or per kilowatt of capacity) by the system’s total renewable and battery capacity (Carrara et al., 2020; Elshkaki & Hilali, 2021; Davis, 2021; Dunn, 2022). I then normalise these totals to t/GWh and t per 1,000 t LCE to make results comparable across sites and countries with different scales and electricity intensities.

3.4.2 Land-use

To quantify the spatial footprint of each scenario, I employ benchmark land-occupation factors expressed in square metres per kilowatt of installed capacity (m²/kW). Multiplying these per-kilowatt figures by the system’s capacity yields the total area occupied. For the wind turbines the direct land transformation was calculated. I report land both as hectares per GWh delivered and

hectares per 1,000 t LCE to make results comparable across sites and countries with different scales and electricity intensities.

3.4.3 Lifecycle GHG emissions

I estimate lifecycle greenhouse-gas emissions by applying published emission-factors (grams CO₂-equivalent per kilowatt-hour or per kilowatt) to each system's total energy delivery or capacity. These emission factors come directly from a variety of sources (Appendix E.) each with its own system boundary and allocation methodology. I have not further harmonized these differing scopes or allocation rules, so the resulting CO₂-equivalent estimates for each technology are not strictly apples-to-apples. In the 3 h scenarios, I also include additional CO₂ from burning diesel to meet 2 % of their energy requirements. Emission factors are used as-published, without reconciling methodological inconsistencies, and therefore my calculated burdens carry the limitations inherent to each original study's boundary and allocation choices. Multiplying these per-unit values by the system's installed capacity yields the total CO₂-equivalent burden. By using fossil and grid emissions factors, I calculated the CO₂ emissions of the sites (in the scenarios that they use diesel or grid only) and then I calculated CO₂ reduction of each site and scenario.

3.5. Sensitivity analysis

To quantify the robustness of the economic results I conducted three complementary analyses:

3.5.1 Key parameters sensitivity

For PV CAPEX, the baseline is 758 \$/kW with bounds 691 and 1000 \$/kW (IRENA, 2022). Wind CAPEX bounds of 1041–1800 \$/kW capture the global weighted-average lower costs and the upper end seen in high-cost markets (IRENA, 2024). Battery CAPEX lower and upper bounds taken from the IRENA-reported range of 139 and 339 dollars per Kwh (IRENA, 2025). Discount-rate bounds of 3–10% follow IEA/NEA (2020), while in the model I use 5% for OECD and 7.5% for non-OECD cases per IRENA (2022). For diesel prices I apply –40% and +30% around each baseline, reflecting the large downshifts seen in 2014–2015 and 2020 (Baffes et al., 2015; World Bank Group, 2020). Similar for

grid tariffs I apply –30% and +50%, consistent with the broad tariff declines in 2023–2024 and plausible future surges from supply or weather shocks (Eurostat, 2024; IEA, 2025). The full set of parameters applied in the sensitivity analysis is summarized in Table 4.

Table 4 Input parameters for sensitivity analysis

| Parameter | Baseline | Lower bound | Upper bound | Citation |
|--|-----------------------------|---------------------|---------------------|--|
| Battery CAPEX (\$/kWh) | 273 | 139 | 339 | IRENA (2022, 2025) |
| Discount rate (%) | 5 (OECD), 7.5 (non-OECD) | 3 | 10 | IRENA (2022); IEA/NEA (2020) |
| PV CAPEX (\$/kW) | 758 | 691 | 1000 | IRENA (2022, 2024) |
| Wind CAPEX (\$/kW) | 1160 | 1041 | 1800 | IRENA (2022, 2024) |
| Diesel electricity price (\$/kWh) | Country-specific | 0.6× base (–40%) | 1.3× base (+30%) | GlobalPetrolPrices.com (2025); Baffes et al. (2015); World Bank (2020) |
| Grid electricity price (\$/kWh) | Site-specific | 0.7× base (–30%) | 1.5× base (+50%) | GlobalPetrolPrices.com (2025); Eurostat (2024); IEA (2025) |

3.5.2 Energy-Source Sensitivity Analysis

The methodology assigns each mine’s electricity to either grid or diesel based on some assumptions. To bracket the effect of this classification, I performed two “what-if” supply scenarios for all sites:

- All-Diesel Case: 100 % of the sites have their electricity supplied by diesel generators.
- All-Grid Case: 100 % of the sites have their electricity supplied by the local grid.

The mean changes in LCOE, IRR, discounted payback period and NPV per tonne under the 100 % diesel and 100 % grid scenarios were calculated relative to the baseline mixed-supply case to quantify the economic impact of energy sourcing assumptions.

3.5.3 Mine-Life Sensitivity

Finally, I examined the effect of project life assumptions by comparing the baseline 20-year mine life against 10-year and 5-year horizons. For each life span, the model outputs (LCOE, IRR, payback, NPV per tonne) were averaged and the differences from the 20-year case plotted in tornado charts. Because a substantial number of sites exhibited “no payback” cases that are excluded from the mean calculations the tornado figures also annotate how many projects in each life-span scenario failed to achieve a usable payback or IRR. This allows direct comparison of how many sites are non-viable under 20-, 10- and 5-year assumptions.

3.5.4 Optimized hybrid renewable system

In order to see how much the results differ when not using the optimized solar–wind hybrids reported by Tong et al. (2021), I performed a sensitivity analysis comparing optimized hybrids (3 h and 12 h storage) with non-optimized counterparts at the same storage duration, and then compared these outcomes with my own scenario results. In the non-optimized dataset, results are reported separately for PV-only, wind-only, and uniform 50:50 hybrids, while the optimized dataset applies country-specific fractions from Tong et al. (2021) to generate hybrid configurations.

The optimized dataset was restricted to the seven countries (China, Australia, Argentina, Brazil, Chile, Canada, and the United States) due to data availability, while the non-optimized dataset covered all ten countries, including Portugal, Mali, and Zimbabwe. From each dataset I calculated the share of sites meeting key investment thresholds (IRR > 10%, NPV per tonne > 0, and positive discounted payback) as well as medians for IRR, NPV/t, payback, and LCOE.

3.6 Assumptions and Limitations

There are multiple assumptions made throughout this report. This analysis applies global-average capital and O&M costs for photovoltaic, wind and battery technologies across all 39 sites, with renewable capacity factors drawn from national or regional averages rather than site-specific meteorology. I assume each mine's operational lifetime matches that of its primary renewable technology and adopt a ten-year lifespan for all battery systems (reflecting the typical 7 – 15-year range). I use a real discount rate of 5 % for OECD and 7.5 % for non-OECD countries. Historical grid and diesel tariffs from 2022 are used to infer 2024 electricity consumption, while the most recent prices inform projected savings under the new systems. I apply country-specific electricity-consumption benchmarks (kWh /LCE) for brine operations where available; where data are absent, I default to 1 200 kWh /LCE. I classify mines as grid- or diesel-supplied by comparing the benchmark-derived cost per LCE to the reported cost per LCE, and assume a generator efficiency of 35 % in all-diesel scenarios.

One of the limitations of the study is that I rely on global averages and regional proxies for costs, capacity factors, and tariffs, so I do not capture local cost fluctuations, project-scale economies, or site-specific resource variability. I address uncertainty only via a deterministic, one-at-a-time tornado sensitivity on six cost and financial parameters, while a full probabilistic Monte Carlo analysis, needed to capture joint and non-linear effects and tail risks, is left for future work. I do not model component degradation, inflation or future escalation of conventional energy prices, which likely leads to conservative estimates of avoided costs. No end-of-life salvage or redeployment value is assigned, and policy instruments such as carbon pricing or emissions credits are excluded. The rule used to assign grid versus diesel supply is approximate, so “mixed” sites may behave differently in reality. Finally, I fix a 20-year project horizon, which overlooks mines with shorter remaining lives, where lifespans under ten years severely hamper project viability.

4. Results

4.1 Technoeconomic results

Table 4. Median values and ranges of techno-economic metrics across all mining sites and scenarios

| Metric | Median | Range (Min–Max) |
|---------------------------|--------|-----------------|
| LCOE (\$/kWh) | 0.123 | 0.070 – 0.171 |
| IRR (%) | 17.56% | -4.21% – 49.36% |
| Payback (years) | 5.04 | 2.19 – 19.60 |
| NPV per t LCE (\$/t) | 667 | -783 – 4,316 |
| Share with IRR \geq 10% | 65.0% | — |

By taking a first glance in table 4, which shows the median value of key metric across all scenarios and sites, key metrics results vary significantly from the median. The wide spreads from the medians because outcomes are strongly shaped by the differences of the input values of each scenario. First, baseline energy price sets the size of avoided-cost cash flows: diesel or high-tariff grids push returns up; cheap grids pull them down (Bitaraf & Buchholz, 2018; Ellabban & Alassi, 2021; Issa et al., 2023). Second, storage duration trades reliability for cost: moving from short to long BESS raises CAPEX and typically LCOE, lengthening payback (Maronga et al., 2021). Third, resource quality varies by site: capacity factors shift annual generation and net savings, widening both LCOE and IRR (Paneri et al., 2021; Li et al., 2024).

However, consistent with Bitaraf & Buchholz (2018) and Issa et al. (2023), our first results show that incorporating a renewable energy system into a mine can raises returns at today's tech costs and the price of electricity can be lower than the baseline. We adopt 10% as the benchmark IRR, meaning that projects are considered valuable for investors only when $IRR > 10\%$ (Wang et al., 2020). Overall, across all scenarios, 65% of all mining sites have an IRR higher than the 10% threshold, with a median IRR of 17.6% (–4.2% to 49.4%). Only 59 cases out of the 234 site–scenario combinations studied fail to pay back the initial investment within the 20-year horizon, while the median payback time is 5 years. In this report, all scenarios that did not pay back the investment correspond to sites that would receive electricity from the grid, which is much cheaper than electricity generated by diesel. The median LCOE is \$0.123/kWh and in 74.8% of the scenarios (74.8%) the LCOE is below the site's baseline price.

4.1.1 System scale and feasibility

Across 39 off-grid sites, my systems span PV 0.003–1.239 GW, wind 0.002–0.783 GW, and BESS (12 h) 0.008–3.212 GWh to serve 4.1–1,594.6 GWh per year (mean power 0.00047–0.182 GW) (Figure 2; Figure 1). Relative to real mining integrations, typically tens of MW of PV/wind with tens of MWh of BESS, most of my designs are larger, especially storage, mainly because I size for 100% off-grid coverage rather than partial displacement. Moreover, scale explains part of this: production spans 0.4–200 kt LCE per year, with 5 sites 60 kt (including 200 kt and 164 kt) where hundreds or even thousands of MW/MWh of solar panels, wind turbines and BESS are needed. In many sites the generation size is not the problem, but the main constraint is storage: multi-GWh (12 h) batteries are beyond current mining precedents (Figure 1). Smaller and mid-tier producers (30 kt LCE per year) align more closely with today's deployments (tens of MW, 0.1–0.2 GWh BESS). At high-demand sites, meeting 100% of power needs with renewables can require up to 3 GWh of battery storage, bigger than many of the largest BESS projects worldwide (Jessen, 2025). PV and wind builds can reach 1 GW, comparable to flagship projects (Jessen, 2025; Figure 2). Although the techno-economic results are favourable for most sites, the technical feasibility of the biggest energy systems remains uncertain and should be examined in future work. Detailed results are provided in Appendix G (Table G.1).

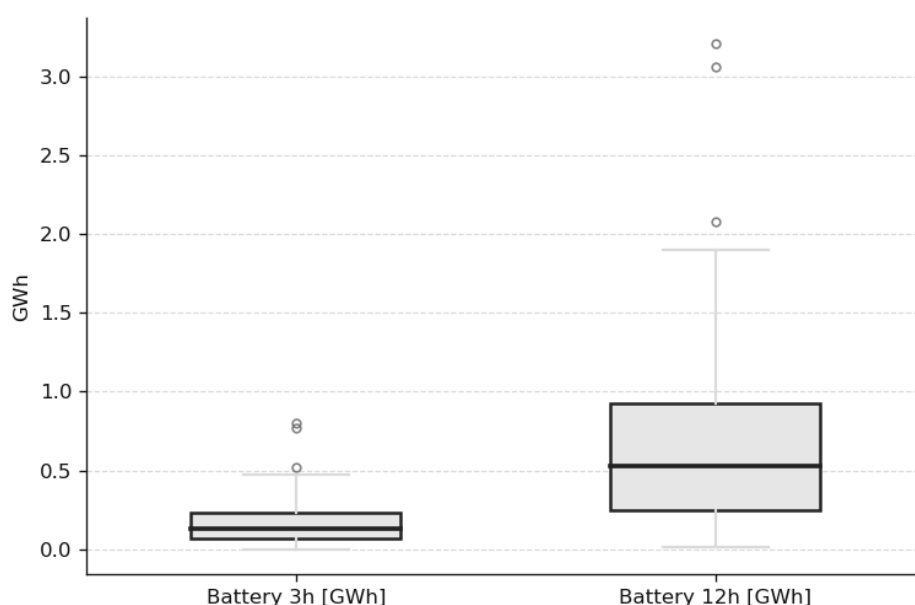


Figure 1. Distribution of battery storage needs across mining sites, showing medians, quartiles, and outliers

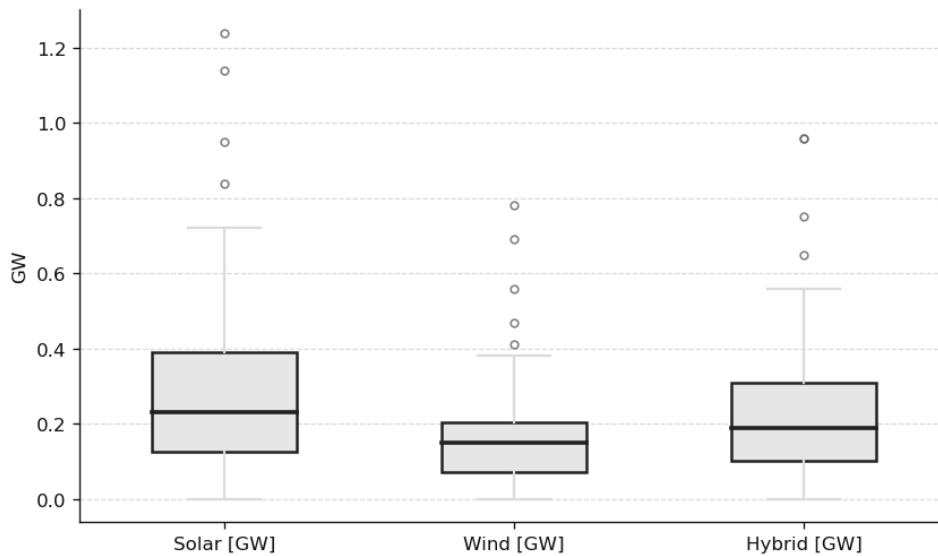


Figure 2. Distribution of installed generation capacities across mining sites, showing medians, quartiles, and outliers for solar, wind, and hybrid systems

4.2 Technoeconomic key metrics across scenarios

Figures 8,9,10 and 11 below depict box-and-whisker distributions for 4 key techno-economic indicators based on scenario. Net present value per tonne of LCE, payback period, internal rate of return and levelized cost of energy across six renewable-plus-storage configurations (hybrid 3 h, hybrid 12 h, PV 3 h, PV 12 h, wind 3 h, wind 12 h).

4.2.1 Effects of storage duration

Extending storage from 3 h to 12 h shifts the medians in a consistent negative way: LCOE increases by \$0.053–0.059/kWh (Figure 12), IRR falls by 9.4–10.3 percentage points (Figure 11), discounted payback lengthens by 1–1.5 years, and NPV per tonne declines by about \$209/t (Figure 9) across PV, wind, and hybrid. Because storage energy capacity scales directly with hours of coverage, extending duration materially increases BESS CAPEX and replacements, while avoided-cost inflows change little between 98% and 100% supply; the larger battery therefore pushes annualised cost up and weakens returns.

In comparing storage durations, systems configured with 3 h battery capacity consistently demonstrate superior techno-economic performance relative to their 12 h counterparts. Median

LCOE is substantially lower (0.087 \$/kWh vs. 0.146 \$/kWh), and a greater proportion of sites achieve positive net present value (80% vs. 64%) and investment-attractive returns (IRR > 10% in \approx 73% vs. 56%). Furthermore, short-duration storage allows the majority of projects to undercut prevailing grid or diesel tariffs (85% vs. 64%). These findings underscore a clear trade-off: while long-duration storage enhances system autonomy, it imposes a significant economic penalty, thereby narrowing the pool of viable projects.

4.2.2 Effects of technology

Within-scenario technology choice shifts the medians in a consistent way across all metrics with 100% wind and 3h storage scenarios performing better. Wind posts the lowest median LCOE at both storage levels (3 h \approx 0.084 \$/kWh; 12 h \approx 0.137 \$/kWh), with Hybrid close behind and PV slightly higher (Figure 12). Wind produces more energy per installed kW, cutting required capacity and spreading fixed costs. The hybrid scenario mixes the two profiles and naturally falls in the middle. And even though PV is cheaper per kW, that price advantage alone isn't enough to offset wind's higher output per kW. Under 3 h scenarios, wind also leads on returns, highest median IRR (\approx 24–25%), highest median NPV/t (\approx \$0.7 k/t), and the shortest median payback (4.4 y) (Figures 11, 9, 10 respectively). More kWh per kW means larger avoided-cost cash flows for the same spend, so IRR and NPV climb and payback shortens.

However on the likelihood of having cheaper electricity cost per kWh (LCOE) than the conventional (baseline) supply, Hybrid-3 h performs best (about 87% of sites). Wind-3 h and PV-3 h are essentially tied, each at 84.6% of sites. This higher frequency reflects the hybrid's averaging of PV and wind across heterogeneous sites, which reduces the risk of leaning entirely on a locally weak resource and increases the chance of pricing below the baseline.

In the 12 h set, technology effects compress even more: medians converge near 14% IRR, paybacks cluster around 5.0–5.4 y, and LCOE distributions sit higher with little separation among PV, wind, and hybrid (Figures 11, 10, 12); all three show the same shares of around 65% having IRR \geq 10% and LCOE below baseline, and each records 14 no-payback cases (Figure 10). Overall, technology only shifts the results slightly, while storage duration is the main factor driving differences in LCOE, IRR, NPV per tonne, and payback.

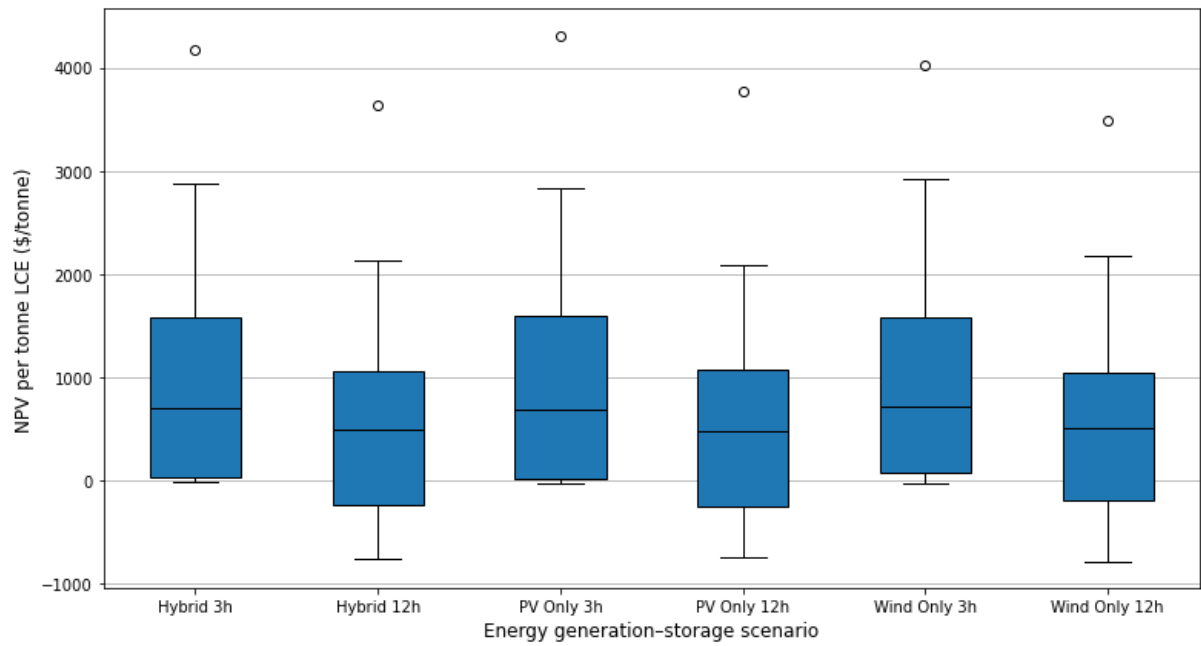


Figure 3. Distribution of net present value per tonne LCE across energy generation–storage scenarios, showing medians, quartiles, and outliers.

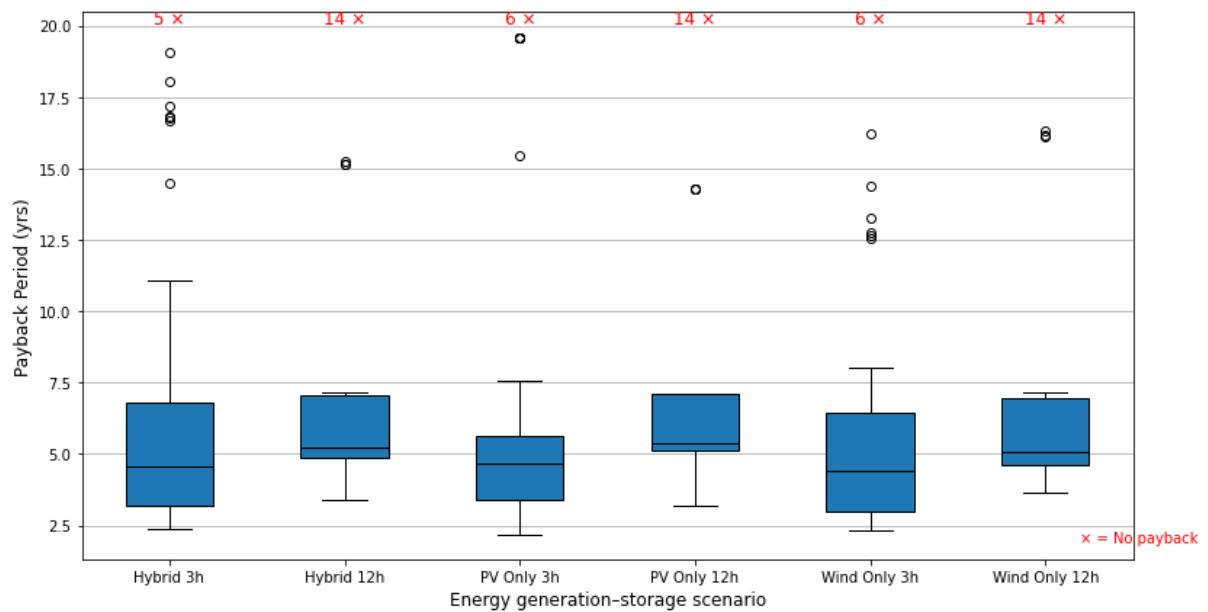


Figure 4. Distribution of payback periods across energy generation–storage scenarios, showing medians, quartiles, and outliers (x = no payback)

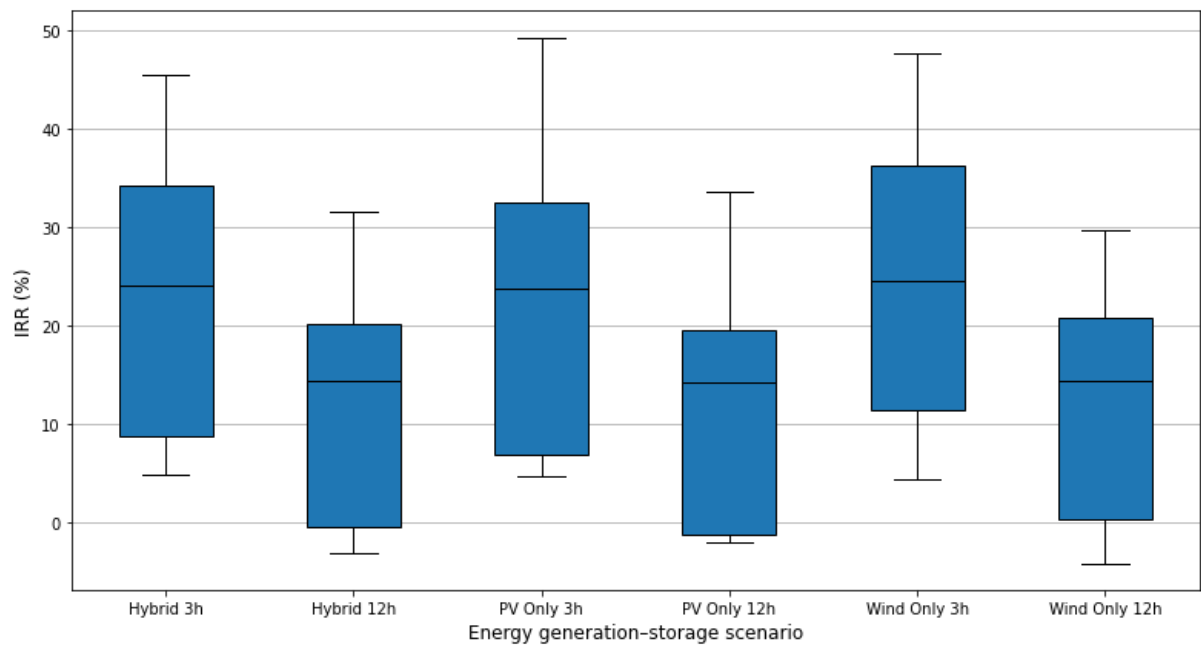


Figure 5. Distribution of internal rates of return (IRR) across energy generation–storage scenarios, showing medians, quartiles, and outliers

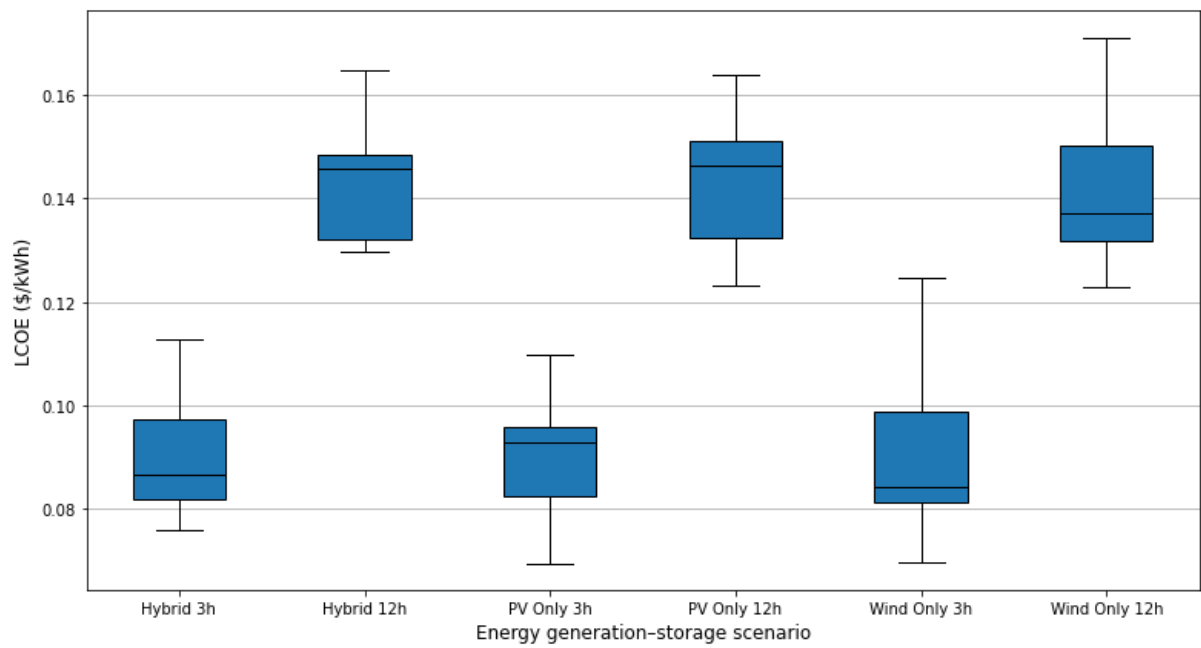


Figure 6. Distribution of levelized cost of energy (LCOE) across energy generation–storage scenarios, showing medians, quartiles, and outliers

4.3 Technoeconomic findings by country

Because the number of sites varies widely, China (11), Australia (9), Argentina (5), Brazil (4), Zimbabwe (3), Chile (3), and one each in Canada, Portugal, Mali, and the United States, comparisons are inherently more robust for countries with many sites and may be less representative for those with only a single location. In the figures a wide spread on the separate results of each country driven by the fact that half of the scenarios have 4 times more storage capacity and due to limited sites per country. Before interpreting these results, it is also important to consider production capacity. Not all countries contribute equally to the available lithium supply: Australia, Chile, and China together account for roughly three-quarters of modelled production. Zimbabwe and Argentina are medium contributors (1/6 of total production combined), while Brazil, Canada, and Mali represent a smaller share (approximately 7%). The United States and Portugal contribute less than 1%, and although their results can be extreme, they have little importance overall.

4.3.1 Levelized cost of energy and scale effects by country

As shown in figure 13, the median LCOE's per country differ $\approx 0.06/\text{kWh}$ between the lowest recorder in the United States ($\approx \$0.10/\text{kWh}$) and the highest in Zimbabwe ($\approx \$0.16/\text{kWh}$), Mali ($\approx \$0.16/\text{kWh}$). Within the countries the big difference is driven by the different capacity storage between scenarios which raises significantly total initial investment. Against each country's baseline energy price, every scenario in Australia, Chile, Portugal, Zimbabwe, and Mali have LCOE below the baseline. Brazil and China also perform strongly, with 75% and 62% of scenarios, respectively, beating the baseline. In contrast, Argentina underperforms: only 33% of its scenarios have an LCOE below the baseline, meaning that the electricity produced by the system is costlier than conventional energy. This is driven mainly by Argentina's cheaper grid electricity and the high LCOE values under the 12 h scenarios.

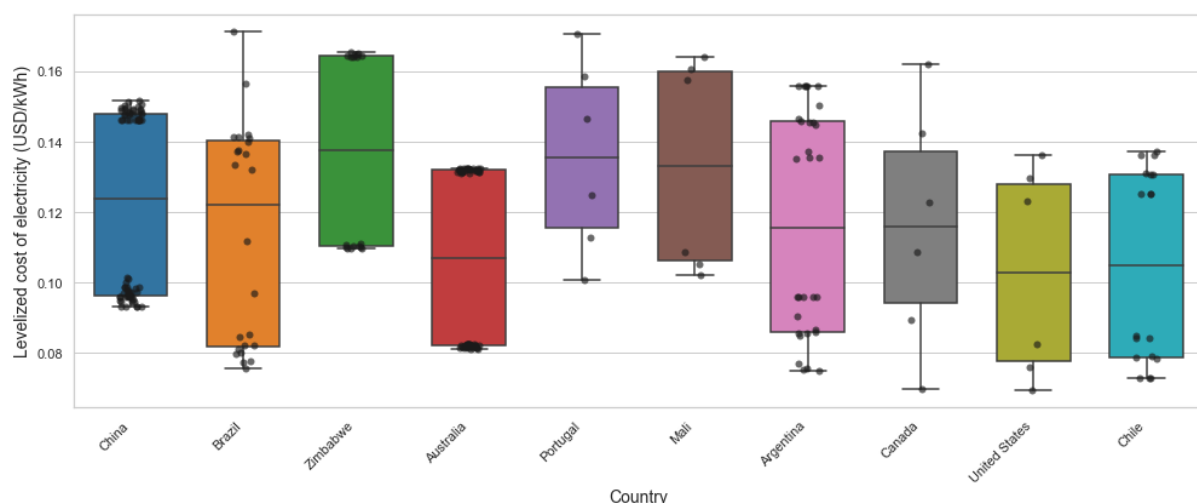


Figure 7. Distribution of levelized cost of electricity (LCOE) across countries, showing medians, quartiles, and outliers

4.3.2 Payback period by country

Figure 14 shows that across countries, the median payback spans from 2.9 years in Portugal and 3.4 years in Zimbabwe to 17 years in Argentina and the United States. Mid-range medians include Brazil 4.7, Mali 4.0, Australia 4.4, China 5.8, Chile 10.4, and Canada 11.6.

The median payback period for most countries is low indicating a healthy investment, but we should take into account that those values are medians calculated by the scenarios that actually paid back. Many sites had scenarios that did not paid back in the assumed 20 year life span of the mines. Argentina and China had 20 and 25 of the total 30 and 66 respectively. While Australia, Chile, Mali, Portugal, and Zimbabwe have no no-payback cases. Payback time is significantly affected by the energy savings (from conventional energy not being bought), the country-specific energy price is a major driver, as it is the only positive cash flow. All the scenarios that did not paid back the investment was compared to a site with grid connection. Though there are exceptions, for example, some sites in Argentina can achieve payback under the right configuration, but the payback period is so long that it approaches the mine's operating life. Moreover all the sites in Chile are connected with Grid and manage to achieve a median payback of approximately 10 years.

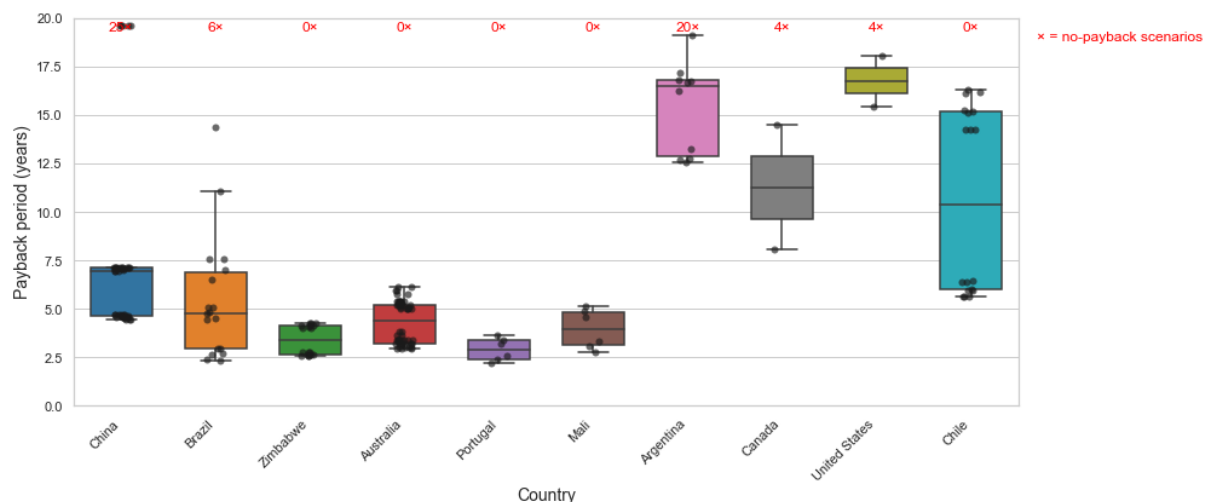


Figure 8. Distribution of payback periods across countries, showing medians, quartiles, and outliers (x = no payback)

4.3.3 Net present value by country

The median NPV per tonne of LCE is positive for most countries. Especially, Portugal and Mali post the highest median NPVs ($\approx \$3,905/\text{t}$ and $\approx \$2,508/\text{t}$), followed by Zimbabwe ($\approx \$1,336/\text{t}$) and Australia ($\approx \$1,135/\text{t}$). Mid-pack countries include China (median $\approx \$508/\text{t}$), Brazil ($\approx \$372/\text{t}$), and Chile ($\approx \$323/\text{t}$). The countries with negative NPV/tonne LCE are Canada ($\approx -\$80/\text{t}$), Argentina ($\approx -\$87/\text{t}$), and the United States ($\approx -\$112/\text{t}$). The net present value is influenced by the positive inflows (energy savings) and negative outflows of cash (capex, o&m, replacements). In addition to medians, the share of scenarios with NPV > 0 shows how consistently each country performs: Australia, Zimbabwe, Portugal, Mali, and Chile are 100% positive across scenarios. Brazil and China sit in the middle with 75% and 55% respectively. While Canada with 33%, United States with 33%, and Argentina with 30% sit at the lower end.

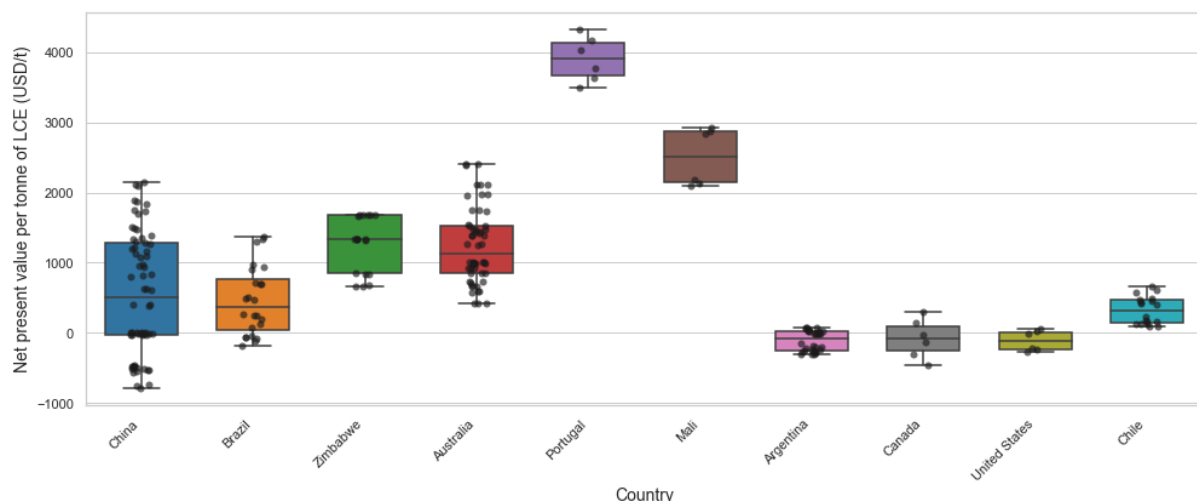


Figure 9. Distribution of net present value per tonne LCE across countries, showing medians, quartiles, and outliers

4.3.4 Internal rate of return by country

Portugal and Zimbabwe have the highest IRRs (about 35–40%), followed by Mali (30–35%) and Australia (25–30%). Brazil and China vary substantially by site; Chile sits in the mid-teens. Argentina, Canada, and the United States are near zero, with several cases below zero. All modelled cases in

Australia, Portugal, Mali, and Zimbabwe exceed the 10% IRR threshold, while the shares are 75% in Brazil, 55% in China, 50% in Chile, 17% in Canada, 13% in Argentina, and 0% in the United States. Since there are non other returns than the assumed energy the mine otherwise would buy, IRR is higher in countries with sites relying on diesel or expensive energy. It also improves where the system delivers more energy due to stronger wind/solar resource.

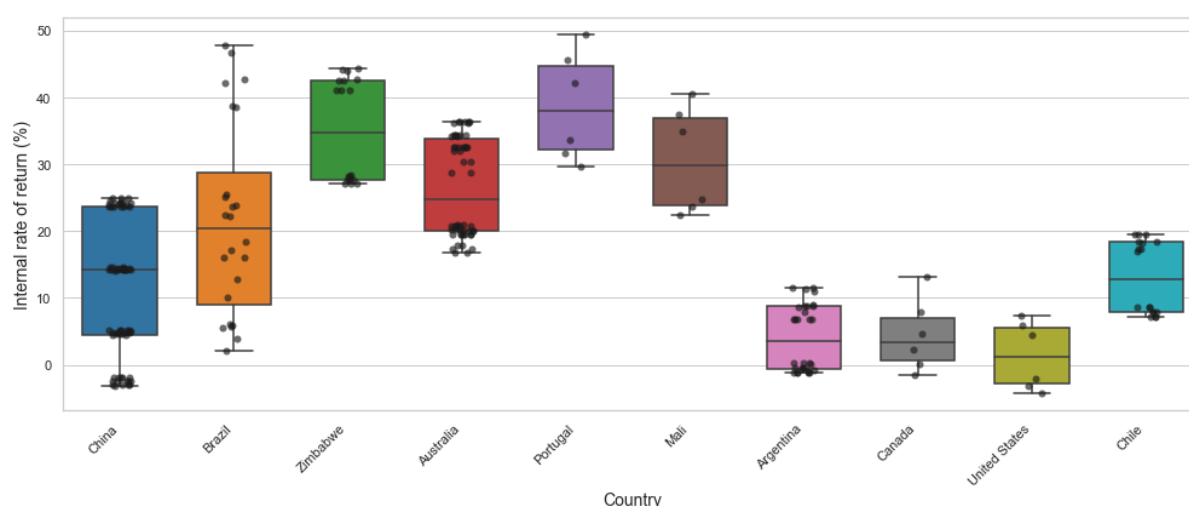


Figure 10. Distribution of internal rates of return (IRR) across countries, showing medians, quartiles, and outliers

Countries with stronger solar or wind capacity factors, higher baseline diesel or grid prices, and lower electricity intensity tend to exhibit lower LCOE, shorter payback, higher NPV, and higher IRR. Higher capacity factors raise annual MWh for the same capital stock, higher energy prices increase avoided-cost cash flows, lower electricity intensity reduces required system size and energy, shorter storage reduces capital intensity. Moreover a lower discount rate (oecd countries) lowers annualized cost and raises present value returns (IRENA., 2022).

4.4 Environmental impact

4.4.1 Land use

I report land transformation both per unit of energy (ha/GWh) and per unit of output (ha per 1,000 t LCE) (Table 5; Table 6). Across scenarios, land intensity follows a stable technology hierarchy, with solar photovoltaic systems having the highest values, followed by hybrid systems, and wind systems the lowest (medians: 0.0494, 0.0349, 0.0246 ha/GWh). This ranking also carries through to the per-tonne metric. Cross-country variation is explained by capacity factors and processing intensity, not

mine size since the results are normalized: Mali, Portugal, and China sit highest, while Brazil and the United States are lowest. Practically, spatial footprint is minimized by technology choice and site resource quality (which set ha/GWh), while the per-tonne footprint additionally reflects processing energy intensity which scales ha per 1,000 t but not ha/GWh. Typical lithium-site footprints range from the low hundreds of hectares for hard-rock operations to the low-thousands for brine-evaporation systems, reaching 4,200 ha at Salar de Atacama (Torres et al., 2024). My renewable-plus-storage systems (PV, wind, and BESS) have a land-transformation range of 1.5 to 1,430 ha, meaning that if these installations cannot be hosted within the already transformed mine area, a significant amount of additional land (equal to the entire mine's footprint) will be needed.

Table 5 Land use intensity by energy generation–storage scenario, expressed per 1,000 t LCE and per GWh delivered

| Scenario | ha/1000 t LCE | ha/GWh delivered |
|-----------------|----------------------|-------------------------|
| Solar | 12.26 (4.84–28.80) | 0.0494 (0.0396–0.0705) |
| Wind | 5.94 (2.34–14.45) | 0.0246 (0.0169–0.0381) |
| Hybrid | 9.10 (3.59–21.33) | 0.0349 (0.0282–0.0481) |

Table 6 Land transformation intensity by country, expressed per 1,000 t LCE and per GWh delivered annually.

| Country | ha/1000 t LCE | ha/GWh delivered annually |
|----------------------|----------------------|----------------------------------|
| Argentina | 6.18 (2.52–9.41) | 0.0338 (0.0178–0.0494) |
| Australia | 8.50 (2.34–19.83) | 0.0349 (0.0227–0.0470) |
| Brazil | 5.81 (2.53–10.97) | 0.0294 (0.0169–0.0396) |
| Canada | 11.83 (5.11–18.55) | 0.0450 (0.0194–0.0705) |
| Chile | 6.70 (4.73–11.04) | 0.0330 (0.0246–0.0412) |
| China | 14.31 (4.41–28.21) | 0.0440 (0.0297–0.0581) |
| Mali | 21.06 (13.33–28.80) | 0.0402 (0.0254–0.0548) |
| Portugal | 18.12 (14.35–21.90) | 0.0481 (0.0381–0.0581) |
| United States | 5.05 (3.87–6.23) | 0.0321 (0.0246–0.0396) |
| Zimbabwe | 6.99 (3.50–13.69) | 0.0414 (0.0279–0.0548) |

4.4.2 Material consumption

For the interpretation of these results, I normalized in the same way as for land transformation: per unit energy (t/GWh) and per unit output (t per 1,000 t LCE). I use material intensity as a design and risk indicator. It highlights where the bill of materials is concentrated and how technology mix and storage size shift that exposure. These intensities reflect annualized capital material requirements (20-year system life assumed), normalized against annual LCE output and annual electricity delivered (GWh) (Tables 7–8; Appendix H, tables H.1–H.4).

By scenario, storage predominantly scales battery materials: moving from 3 h to 12 h increases lithium from 0.031 to 0.125 t/1,000 t LCE (and from 0.002 to 0.010 t/GWh), with graphite showing the same pattern (Tables 7–8). Technology effects are distinct: PV concentrates aluminium, copper, and silver; wind concentrates neodymium and dysprosium; and hybrid sits between (Appendix H, tables H.1–H.2). Silver appears only in PV, while wind carries Nd/Dy which are unchanged across storage. In PV 12 h as many as 8.61 tonnes of aluminium and 3.68 tonnes of copper would be needed (in an assumed 20-year life span) to produce 1,000 tonnes of LCE yearly. Shifting the scenario to PV 3 h would decrease aluminium to 5.14 tonnes and copper to 2.75 tonnes. In the least material-intensive scenario 1.57 and 0.78 tonnes of aluminium and copper will be used (an 80% decrease in comparison to the PV 12 h scenario) (Table 7).

On a per-GWh basis, countries cluster closely because I use identical PV/wind/hybrid + storage designs across all sites and differences mainly reflect local resource quality (Appendix H, table H.4). Per-1,000-t LCE values spread more because they also reflect electricity intensity of the production route: higher values in energy-intensive Mali (Al ~10.97; Cu ~3.88 t/1,000 t) and Portugal (Al ~8.22; Cu ~3.06) versus lower values in Argentina (Al ~3.51; Cu ~1.19) and Brazil (Al ~3.23; Cu ~1.26) which have many lesser energy-intensive brine operations (Appendix H, table H.3). The difference in material usage per ton of LCE between countries is bigger even than that of different technologies: the renewables energy system aluminium, copper and graphite usage per ton of LCE extracted in the mines in Mali can be 210–280% higher than the mines in United States and Argentina (Appendix H, table H.3).

Table 7 Per Scenario material intensity per 1000 t LCE (medians)

| Scenario | Aluminium | Copper | Graphite | Silver | Neodymium | Dysprosium | Lithium |
|-------------------|-----------|--------|----------|--------|-----------|------------|---------|
| PV 3h | 102.795 | 55.058 | 7.118 | 0.212 | 0.000 | 0.000 | 0.623 |
| PV 12h | 172.232 | 73.677 | 28.473 | 0.212 | 0.000 | 0.000 | 2.493 |
| Wind 3h | 31.394 | 15.633 | 7.118 | 0.000 | 2.533 | 0.412 | 0.623 |
| Wind 12h | 100.622 | 34.252 | 28.473 | 0.000 | 2.533 | 0.412 | 2.493 |
| Hybrid 3h | 45.120 | 20.776 | 7.118 | 0.053 | 0.633 | 0.103 | 0.623 |
| Hybrid 12h | 114.556 | 39.395 | 28.473 | 0.053 | 0.633 | 0.103 | 2.493 |

Table 8 Per Scenario material intensity per GWh delivered annually (medians)

| Scenario | Aluminium | Copper | Graphite | Silver | Neodymium | Dysprosium | Lithium |
|-------------------|-----------|--------|----------|--------|-----------|------------|---------|
| PV 3h | 8.200 | 4.415 | 0.547 | 0.017 | 0.000 | 0.000 | 0.048 |
| PV 12h | 13.530 | 5.844 | 2.186 | 0.017 | 0.000 | 0.000 | 0.191 |
| Wind 3h | 2.464 | 1.260 | 0.547 | 0.000 | 0.211 | 0.034 | 0.048 |
| Wind 12h | 7.794 | 2.690 | 2.186 | 0.000 | 0.211 | 0.034 | 0.191 |
| Hybrid 3h | 3.508 | 1.604 | 0.547 | 0.004 | 0.053 | 0.009 | 0.048 |
| Hybrid 12h | 8.839 | 3.034 | 2.186 | 0.004 | 0.053 | 0.009 | 0.191 |

4.4.3 Greenhouse gas emissions

Extending battery storage from 3 h to 12 h consistently lowers total system CO₂ emissions under both minimum and maximum range (Figure 11). Among the generation options, wind-only configurations yield the smallest lifecycle footprints, hybrid wind-solar systems occupy an intermediate position, and PV-only scenarios incur the highest emissions—reflecting the relatively greater embedded carbon intensity of the production of solar PV components.

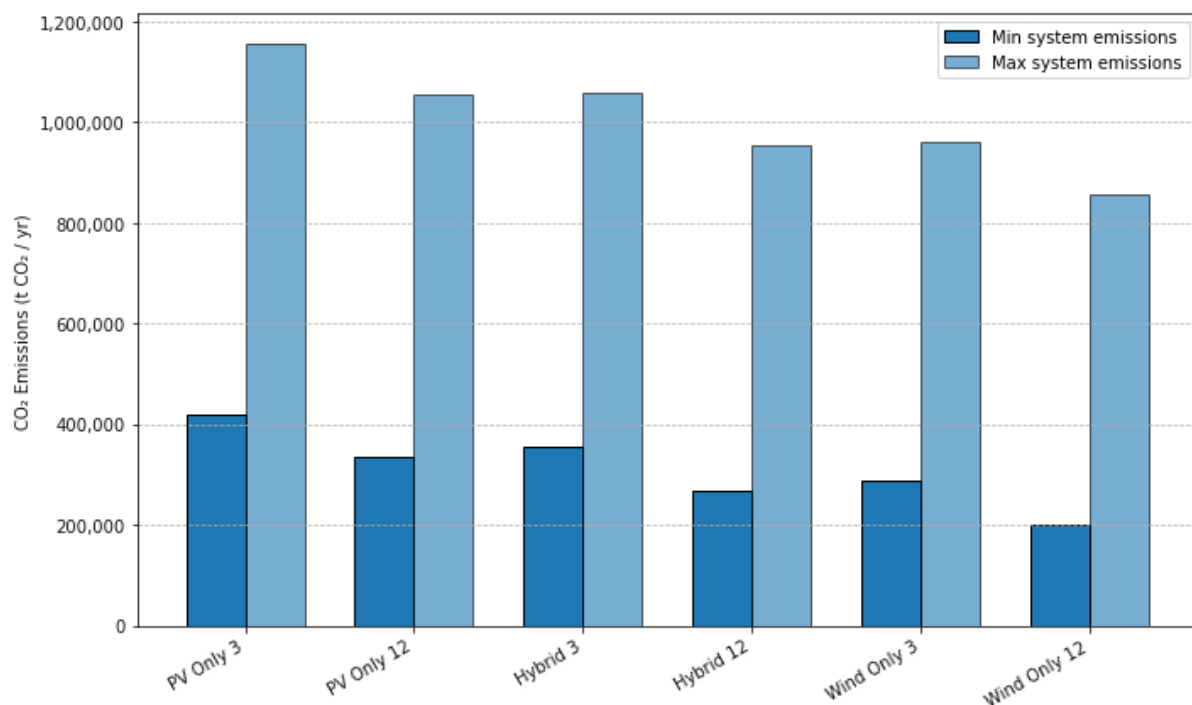


Figure 11. Annual CO₂-equivalent emissions across energy generation–storage scenarios, showing minimum and maximum system values.

When compared to each site’s conventional baseline, all-renewable configurations deliver median CO₂ reductions exceeding 90 %, with 12 h storage systems achieving the greatest abatement since 3 h designs still rely on a 2 % diesel fallback. As illustrated in Figure 12, even under ideal operating conditions a shift to renewables alone leaves residual emissions of 2–4 % in the best case and 6–9 % in the worst case of the original baseline, reflecting life-cycle impacts of equipment manufacture and backup. Although this represents a massive reduction in electricity-related CO₂ output, achieving truly net-zero mining will require carbon-neutral production and supply chains for the renewable generation and storage technologies themselves.

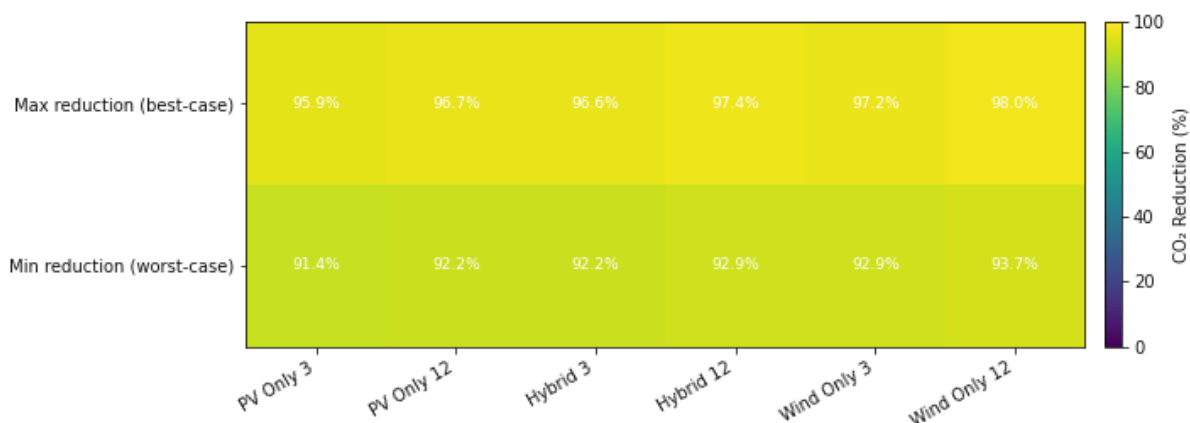


Figure 12. Percentage reduction in CO₂ emissions across energy generation–storage scenarios, showing best-case and worst-case outcomes

4.5 Sensitivity analysis

4.5.1 Robustness of financial performance under parameter variation

Internal rate of return. Diesel price is the dominant driver of IRR. Moving diesel to the lower end reduces the mean IRR by about 7 percentage points, while the upper end raises it by about 5 percentage points. Grid-electricity price and battery CAPEX are the next most consequential levers and each shifts IRR by a few percentage points; wind and PV CAPEX have smaller effects. The discount rate does not change IRR: by definition IRR is the rate that makes NPV equal to zero, so it is independent of whatever discount rate is applied. Overall, operating-cost variables shape returns most strongly, technology CAPEX is secondary, and the discount rate is irrelevant for IRR.

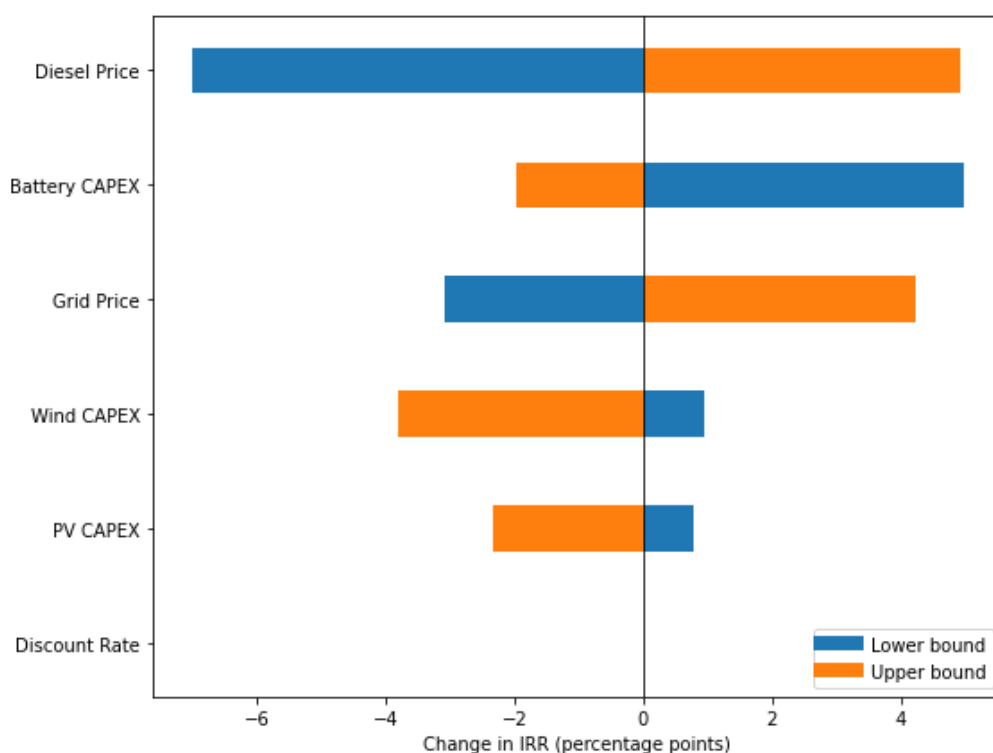


Figure 13. Change in internal rate of return under variation in key parameters

Levelized cost of energy. LCOE is governed primarily by the discount rate and battery CAPEX. Taking the discount rate to its upper end increases LCOE by roughly \$0.03/kWh, while moving battery costs to the low end reduces LCOE by about \$0.02–0.03/kWh. PV and wind CAPEX have smaller yet visible effects, and diesel and grid prices have negligible influence at the scale of a few ten-thousandths of a dollar per kWh. In short, the levelized cost of energy is driven mainly by the upfront capital required and the discount rate, not by fuel prices.

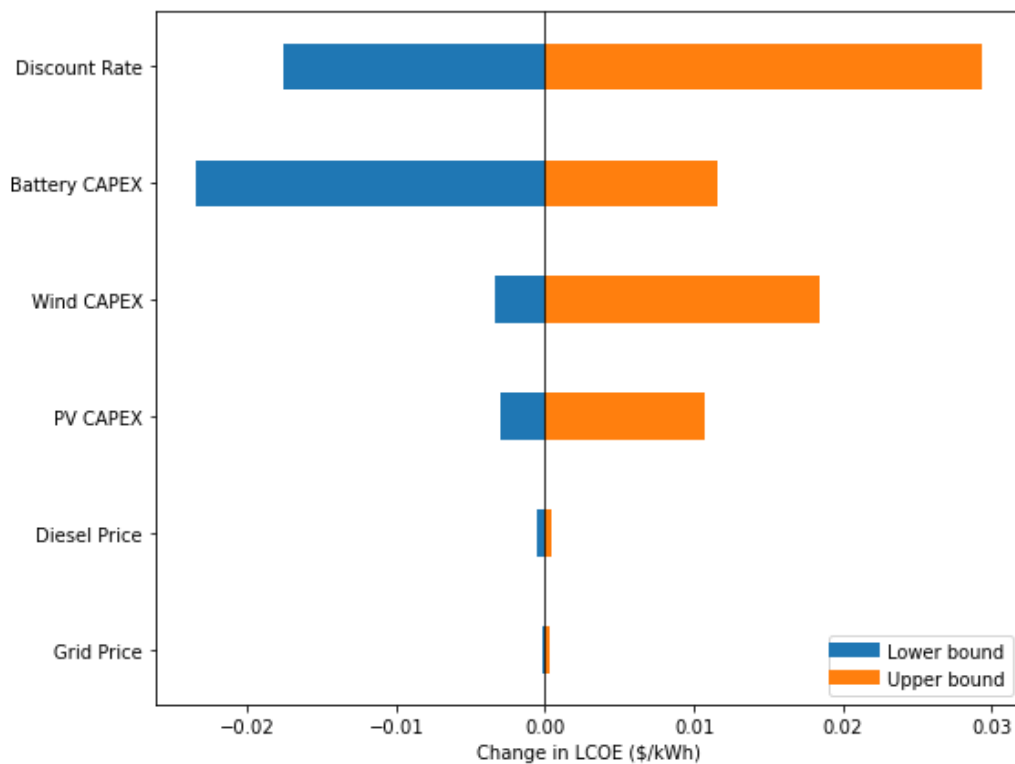


Figure 14. Change in levelized cost of electricity under variation in key parameters

NPV per tonne of LCE. Diesel price again dominates. Across its range, NPV per tonne shifts by approximately $-\$0.5\text{k}$ to $+\$0.4\text{k}$. The discount rate and grid price follow with effects in the order of several hundred dollars per tonne, then battery CAPEX, with PV and wind CAPEX smaller still. This reflects that NPV is driven by avoided energy expenditures.

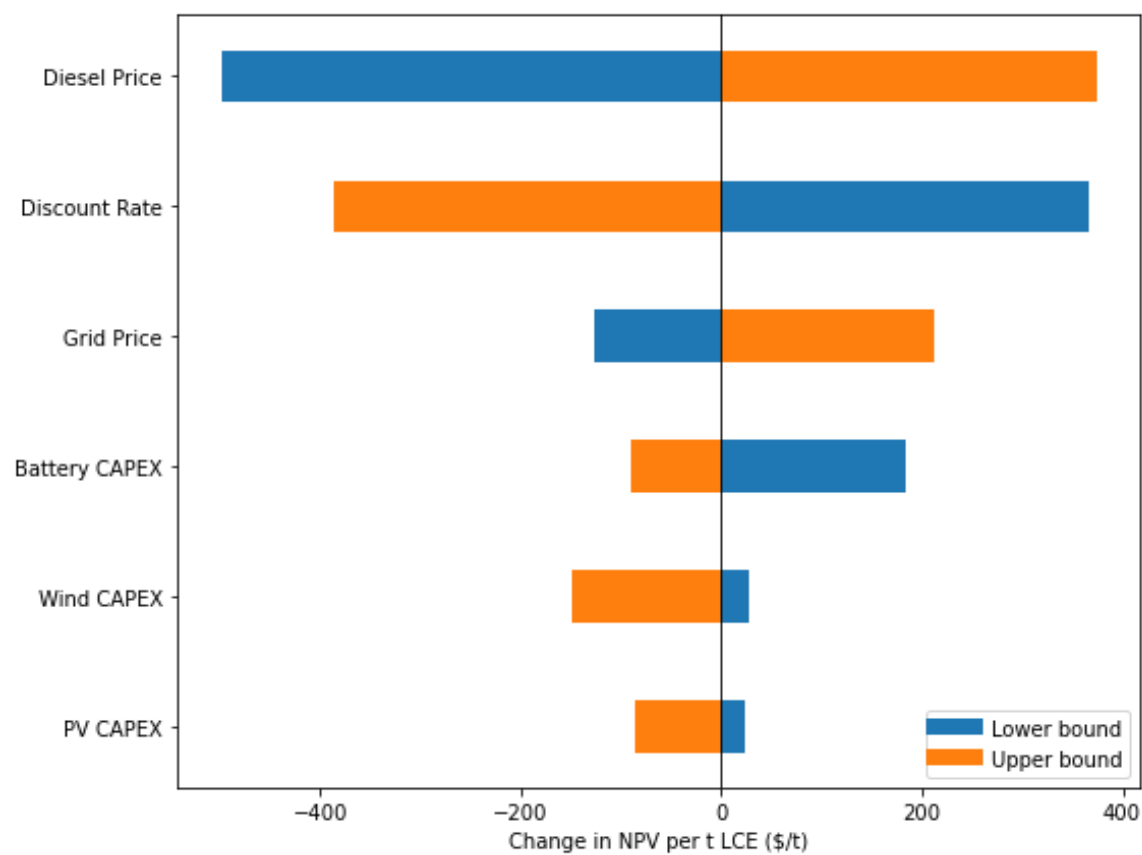


Figure 15. Change in net present value per tonne of lithium-carbonate-equivalent production under variation in key parameters

Payback time. Payback responds most to diesel and grid prices. A high-diesel case shortens payback by about three years, whereas a low-grid case can lengthen it by up to roughly two years. Battery CAPEX and the discount rate typically shift payback by around one year, while PV and wind CAPEX changes are generally sub-year. In viability terms, diesel and grid are the parameters most likely to move configurations across the payback versus no-payback threshold, with battery CAPEX and the discount rate next.

In the baseline, 59 configurations fail to achieve payback. Grid-electricity prices are the dominant lever: a 30 percent decrease increases the non-payback count by 23 (to 82), whereas a 50 percent increase reduces it by 35 (to 24). The discount rate is next in influence: lowering it to 3 percent reduces the count by 28 (to 31), while raising it to 10 percent increases the count by 18 (to 77). Battery capital cost is also material: reducing it to 139 USD per kWh lowers the count by 29 (to 30), whereas increasing it to 339 USD per kWh raises the count by 9 (to 68). Wind capital cost changes have smaller effects, decreasing the count by 11 (to 48) at the lower bound and increasing it by 15 (to 74) at the upper bound. Photovoltaic capital cost changes decrease the count by 7 (to 52) at the lower bound and increase it by 7 (to 66) at the upper bound. Diesel price has a mixed but comparatively small effect: a 40 percent decrease increases the count by 14 (to 73), and a 30 percent increase raises it by 2 (to 61).

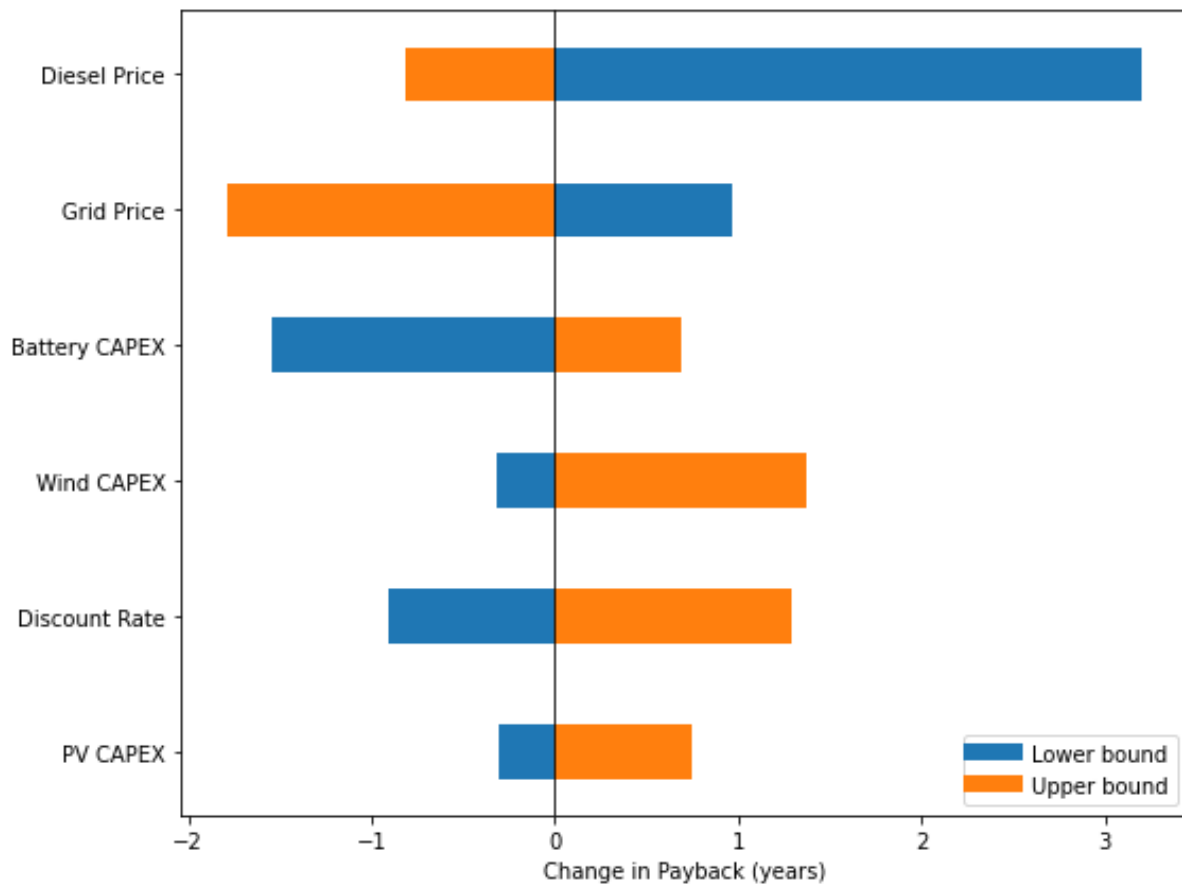


Figure 16. Change in payback period under variation in key parameters (no-payback counts indicated)

4.5.2 Energy-supply assumption robustness

In order to assess the robustness of the baseline assumptions regarding the predominant energy supply at each mining site, I conducted a targeted sensitivity analysis in which all sites were forced to transition exclusively to either grid-electricity or diesel-generated electricity. The figures of the results of this sensitivity analysis can be found in Appendix C. In the original scenario, each mine was assigned to its most-likely primary energy source, either grid or diesel, and 59 mines failed to achieve payback within the project horizon. Under the “All-Grid” assumption, the mean levelized cost of energy (LCOE) changes only slightly, while the “All-Diesel” assumption produces a similarly small shift. Constraining all sites to grid power also lengthens the average payback time by ~4.95 years and raises the number of non-payback sites from 59 to ~130. By contrast, the diesel-only scenario still lengthens average payback (+2.04 years) but eliminates all non-payback incidents (0

sites). In terms of project value, the “All-Grid” case reduces mean net present value per tonne of LCE (NPV/t) by ~US\$584 t⁻¹, whereas “All-Diesel” increases mean NPV/t by ~US\$455 t⁻¹. Finally, average internal rate of return (IRR) declines by ~10.8 percentage points under the “All-Grid” configuration but rises by ~9.35 percentage points under “All-Diesel.” Transitioning lithium mining sites that rely on grid electricity uniformly degrades financial performance—raising effective capital burden through longer payback and creating a larger cohort of non-viable mines—whereas moving to diesel leaves LCOE virtually unchanged but substantially improves IRR and NPV and removes no-payback cases. This pattern reinforces that the assumed conventional energy price is a significant driver of financial viability: where the counterfactual energy is more expensive (diesel), the avoided-cost benefit of renewables is larger.

4.5.3 Mining sites lifespan assumption robustness

To explore the influence of mine operational lifespan on the economic performance metrics, I re-ran the model shortening the assumed project life from the 20-year baseline to 10 and 5 years. Since most of the capital costs are paid up front, shortening the mine’s operating life greatly reduces its value, raises its costs, and lowers its returns. The figures for this sensitivity analysis are in Appendix D.

Projecting a 10-year operating life instead of 20 years reduces mean NPV per tonne of LCE by 304 USD/t; shortening to 5 years yields a mean loss of 1,086 USD/t (Figure D3). In parallel, LCOE increases: with a 10-year life, mean LCOE rises by 0.047 USD/kWh, and with a 5-year life it climbs by 0.119 USD/kWh (Figure D2). Because the same upfront CAPEX is recovered over fewer years and fewer total kWh per tonne, the cost per unit increases when project life shortens. IRR is similarly degraded: a 10-year life reduces mean IRR by 5.44 percentage points, and under a 5-year scenario mean IRR falls by 17.35 percentage points (Figure D1).

Shorter lifetimes raise the share of projects that never pay back, from 59 of 234 (25.1%) at 20 years to 88 of 234 (37.6%) at 10 years and 150 of 234 (64.1%) at 5 years (Figure D4). Among the projects that do pay back, the median payback period becomes shorter when lifespan is reduced (5.02 to 4.73 to 3.45 years), which is expected because the maximum attainable payback is capped by project life, lowering medians even as no-payback cases increase (Figure D4). Taken together, these results demonstrate that assumptions about mine longevity are among the most critical drivers of economic

viability: overly optimistic life estimates can substantially overstate NPV, understate LCOE, and mask the risk of no-payback sites.

4.5.4 Effects of hybrid renewable system optimization on technoeconomic results

At 3 h storage, optimized hybrids do not outperform the uniform 50:50 design or the leading single-technology options (Table 9; Figures 3–6). Median IRR is 17.1%, lower than wind (25%), PV (24%), and uniform hybrids (21%). Median NPV per tonne is 500 USD/t, below PV (700 USD/t) and wind (700 USD/t), and slightly below uniform hybrids (570 USD/t). Payback at 4.9 years is broadly comparable to wind (4.4 years), PV (5.0 years), and hybrids (4.7 years). LCOE at 0.10 USD/kWh is somewhat higher than uniform hybrids (0.080 USD/kWh) but falls within the range of PV and wind. These results show that optimization narrows differences across metrics, but it does not shift hybrids ahead of the strongest PV or wind cases.

At 12 h storage, optimized hybrids perform worse than the uniform 50:50 design and remain weaker than the single-technology systems. Median IRR is 9.9%, compared with 14% for PV and wind and 11.4% for uniform hybrids. Median NPV per tonne is 240 USD/t, well below PV (667 USD/t) and wind (700 USD/t) and only slightly below the uniform hybrid (308 USD/t). Payback extends to 6.6 years, longer than PV (5.0 years), wind (5.4 years), and the uniform hybrid (6.0 years). Median LCOE is 0.16 USD/kWh, higher than all non-optimized options. Thus, under long-duration storage, optimization offers no clear economic advantage, with hybrids remaining less attractive than single-technology alternatives.

These results confirm that optimized hybrids are financially viable under 3 h storage, with a median IRR above 10%, positive NPV in most cases, and median payback within 5 years. However, their performance is weaker than the non-optimized renewable systems. At 12 h storage, optimized hybrids become borderline: the median IRR falls to around the 10% threshold, only about half the sites achieve positive returns, and payback extends well beyond the median values for PV and wind.

Table 9. Median techno-economic performance values of optimized hybrid scenarios (3 h, 12 h, and combined)

| Metric | Optimized 3 h | Optimized 12 h | Optimized all |
|----------------------|---------------|----------------|---------------|
| IRR> 10% (%) | 64.7 | 50.0 | 57.4 |
| NPV/t > 0 (%) | 64.7 | 58.8 | 61.8 |
| Payback achieved (%) | 64.7 | 58.8 | 61.8 |
| Median IRR (%) | 17.1 | 9.9 | 13.0 |
| Median NPV/t (\$/t) | 500 | 240 | 372 |
| Median payback (yrs) | 4.9 | 6.6 | 5.7 |
| Median LCOE (\$/kwh) | 0.10 | 0.16 | 0.13 |

5. Discussion

5.1 Interpretation of key findings

The results show that deploying wind, solar, and BESS to deliver 100% of electricity demand is not worthwhile under current conditions. In practice, what is often reported as 100% reliability is closer to 99.9% for most countries, since there will always be a few days when system reliability cannot be fully met (Tong et al., 2021). Achieving true 100% reliability would require three times overbuild, meaning roughly double the solar and wind capacity compared to the 1.5× factor used here, and even then some countries cannot reach full reliability (Tong et al., 2021). Extending storage from 3 h to 12 h raises LCOE, reduces IRR by 9 to 10 percentage points, and lowers NPV per tonne by 209 \$/t (Figure 12; Figure 11; Figure 9). Material requirements also increase steeply, with lithium and graphite tripling and copper and aluminium rising by 30 to 70% (Tables 7–8; Appendix H, Tables H.1–H.4). The additional emission savings are small, only 5 to 8% beyond the roughly 90% already achieved with 3 h storage, and renewables themselves still carry life-cycle emissions from manufacturing (Dunn, 2022). For mining companies this means that striving for complete autonomy is an expensive strategy with limited environmental benefit. For policymakers it suggests that near-fully renewable systems are a better focus, because almost all of the emission reductions can be achieved without the much higher costs and much higher raw material demands.

The analysis shows that financial outcomes depend significantly on the mine's energy source. In Mali and Zimbabwe, where sites run on diesel, renewables give high IRR and short payback because they replace expensive fuel (Appendix A, Table A1; Figure 13). This indicates that companies should focus integration efforts where avoided costs are highest, while policymakers aiming for wider adoption

must consider carbon pricing or targeted support to make renewables competitive in regions with low-cost grids.

Scaling to the largest operations creates additional challenges. Meeting demand at site which have the highest electricity demand would require near-GW generation and multi-GWh storage, capacities comparable to utility-scale projects yet untested at individual mines (Appendix G, Table G.1). This introduces execution risk and indicates that companies should pursue phased strategies rather than immediate giga-scale deployment. Policymakers, meanwhile, must consider permitting frameworks that can motivate for large renewable infrastructures in mining regions.

Land requirements rise sharply with system size. Median land transformation spans from 0.0246 ha/GWh for wind to 0.0494 ha/GWh for PV (Tables 5–6; Appendix E, Table E2). As mentioned earlier in the land-use results, some renewable systems can occupy areas comparable to the footprint of the mines themselves. This makes it essential for companies to place new systems on land that is already used by mining, while policymakers must set clear land-use rules that balance renewable expansion with biodiversity protection.

Finally, the analysis shows that deeper decarbonization requires substantially more materials. This surge in demand for critical raw materials introduces supply-chain risks for companies and heightens global pressure on resources that are already strategically important. At the same time, solar, wind, and BESS cannot be considered carbon-free technologies, since their production still relies on carbon-intensive supply chains (Dunn, 2022). Decarbonizing these technologies therefore also requires decarbonizing the supply chains of the raw materials they depend on, including aluminium, copper, lithium, graphite, and rare earths. Until this is achieved, solar, wind, and BESS alone cannot deliver net-zero outcomes, and other carbon-free or carbon-neutral technologies should be investigated alongside them.

5.2 Comparison with literature

I find LCOE of \$0.07–0.171/kWh (median \$0.123/kWh), IRR around 17.6% on median (with 65% of cases 10%), and a median payback 5.0 years (but 59/234 cases don't pay back within 20 years).

These results line up with reported projects: the South African hybrid shows IRR 23.5%, payback 4.9 y, LCOE \$0.23/kWh (Nkambule et al., 2023), and the off-grid PV+BESS case shows IRR 16%, payback

5.2 y, LCOE \$0.304 to 0.289/kWh (Bitaraf et al., 2018). Higher LCOE values in these reports are driven by significant usage of conventional energy (Bitaraf et al., 2018; Nkambule et al., 2023). I deliberately test near-full and full renewable electricity supply, and the levelized cost of electricity seems to perform better in comparison to projects with partial renewable integration (Bitaraf et al., 2018; Nkambule et al., 2023). Environmentally, the median CO₂-eq reduction is above 90% versus diesel or carbon-intensive grids, consistent with published mining case studies reporting large operational abatement for South African HRES and for CSP integrated into lithium-brine operations (Nkambule et al., 2023; Dellicompagni et al., 2021).

What's new in this report is that I model two reliability targets: 100% renewable electricity in half of the scenarios and 98% in the other half to test the impact of extra storage on cost and returns, and I compare key techno-economic metrics and environmental impacts across countries. The main outcomes are: moving from 98% (3 h) to 100% (12 h) renewables raises LCOE by \$0.053–0.059/kWh, cuts IRR by 9–10 percentage points, lengthens payback by 1–1.5 years, and reduces NPV per tonne by about \$209, while the incremental CO₂eq reduction is only 5–8% in comparison to 3 h. Land transformation changes only by generation technology, not by storage hours, since the indicators used measure land transformation per kW, not kWh. The difference in land use between technologies is substantial: PV systems require up to 100% more land per unit of energy than wind, with hybrids sitting in between at around 40–45% higher than wind. By contrast, changing storage hours (3 h to 12 h) makes almost no difference for land. Material requirements differ a lot by technology and by storage hours: PV-heavy systems start with more aluminium and copper (plus a little silver), wind uses less Al/Cu but adds rare earths (Nd/Dy), and hybrids sit in between. Increasing storage from 3 h to 12 h doesn't change those tech-specific metals, but it drives battery materials up sharply (lithium and graphite +300%) and also lifts aluminium/copper by roughly 30–70%.

6. Conclusion

This study shows that on-site wind and solar with batteries can power mining sites with electricity at competitive cost while cutting electricity-related CO₂eq emissions by more than ninety percent. Two reliability targets frame the results. With about 3 h of storage and a small (~2%) diesel fuel-only backup, systems deliver near-autonomous supply and generally outperform local diesel or carbon-intensive grids on cost and returns. Pushing to full autonomy with about 12 h of storage removes the

residual diesel but raises capital requirements enough to lift LCOE and weaken IRR and NPV for most sites, while the extra emission savings are small.

Technology choice matters but is secondary to context. Wind tends to post the lowest LCOE and the highest returns; PV's lower \$/kW rarely compensates for lower capacity factors. Geography explains most of the spread: higher conventional energy prices, better renewable capacity factors, and lower electricity intensity of production correlate with lower LCOE, shorter payback, and higher IRR and NPV per tonne. Project lifetime is a decisive filter. The baseline assumes 20 years; shortening life to 10 or 5 years sharply raises LCOE, cuts IRR, and increases the share of no-payback cases. Even with good resources, short-life mines struggle to amortize storage-heavy systems. Scale is a practical constraint at the largest, highest-demand sites. Meeting 100% of load there implies multi-GWh batteries and near-GW generation, which exceed typical mining precedents and warrant staged delivery plans and focused execution risk assessment.

Deeper decarbonization, through longer battery storage, also comes with higher material requirements. Extending storage from 3 h to 12 h increases lithium and graphite demand and raises copper and aluminium needs by 30 to 70%, adding supply-chain risks and intensifying pressure on already critical resources. Moreover, solar, wind, and BESS are not yet carbon-free technologies, since their production still relies on carbon-intensive supply chains. Achieving net-zero mining will therefore require decarbonizing these upstream industries over time, and investigating other carbon-neutral technologies alongside solar, wind, and BESS.

Acknowledgments

I would like to express my gratitude to my two supervisors for their cooperation and guidance. My main supervisor, Dr. Robert Istrate, supported me with weekly meetings and continuous feedback that guided me throughout this project. I am equally thankful to my second supervisor, Dr. Enno Schroeder, who, despite his busy schedule, stepped in when I was struggling to find a second supervisor and made this project feasible.

References

- Abdul Latif Jameel. (2023). Building utility-scale battery storage in Europe: Europe's transition to renewable energy depends on battery storage. Retrieved from <https://alj.com/en/perspective/building-utility-scale-battery-storage-in-europe/>
- Aitken, D., Rivera, D., Godoy-Faúndez, A., & Holzapfel, E. (2016). Water scarcity and the impact of the mining and agricultural sectors in Chile. *Sustainability*, 8(2), 128. <https://doi.org/10.3390/su8020128>
- Anderson, K., Farthing, A., Elgqvist, E., & Warren, A. (2022). Looking beyond bill savings to equity in renewable energy microgrid deployment. *Renewable Energy Focus*, 41, 15–32. <https://doi.org/10.1016/j.ref.2022.02.001>
- Aramendia, E., Brockway, P. E., Taylor, P. G., & Norman, J. (2023). Global energy consumption of the mineral mining industry: Exploring the historical perspective and future pathways to 2060. *Global Environmental Change*, 83, Article 102745. <https://www.sciencedirect.com/science/article/pii/S0959378023001115>
- Arvesen, A., & Hertwich, E. G. (2012). Assessing the life cycle environmental impacts of wind power: A review of analytical approaches. *Renewable and Sustainable Energy Reviews*, 16(8), 6724–6733. <https://doi.org/10.1016/j.rser.2012.07.061>
- Ataei, M., & Barabadi, A. (2023). Integration of renewable energy and sustainable development with strategic planning in the mining industry. *Results in Engineering*, 20, 101412. <https://doi.org/10.1016/j.rineng.2023.101412>
- Baffes, J., Kose, M. A., Ohnsorge, F., & Stocker, M. (2015). The great plunge in oil prices: Causes, consequences, and policy responses (Policy Research Note No. 1). World Bank Group. https://www.worldbank.org/content/dam/Worldbank/Research/PRN01_Mar2015_Oil_Prices.pdf
- Barbose, G., Margolis, R., & Darghouth, N. (2024). Land requirements for utility-scale PV: Update on system footprint and spacing. Lawrence Berkeley National Laboratory. Retrieved from <https://emp.lbl.gov/publications/land-requirements-utility-scale-pv>
- Bitaraf, H. (2018, May). Reducing energy costs and environmental impacts of off-grid mines [Conference presentation]. 3rd International Hybrid Power Systems Workshop, Tenerife, Spain.

https://hybridpowersystems.org/wp-content/uploads/sites/9/2018/05/4B_2_TENE18_007_paper_Bitaraf_Hamideh.pdf

Brady, M. (2020). Energy storage benefit-cost analysis. Clean Energy States Alliance. Retrieved from <https://www.cesa.org/wp-content/uploads/Energy-Storage-Benefit-Cost-Analysis.pdf>

Brown, A., & Montano, P. (2024). Fekola Complex, Mali, NI 43-101 technical report (Effective December 31, 2023). B2Gold Corp. Retrieved from <https://minedocs.com/26/Fekola-TR-12312023.pdf>

Burgess, D. (2012). A method of calculating autogenous/semi-autogenous grinding mill specific energies using a combination of Bond work indices and Julius Kruttschnitt parameters, then applying efficiency factors. *Proceedings of the 11th Mill Operators' Conference* (Hobart, TAS, 29–31 October 2012). Australasian Institute of Mining and Metallurgy (AusIMM). Retrieved from <https://www.ceecthefuture.org/wp-content/uploads/2013/01/Burgess.pdf> [ceecthefuture.org](https://www.ceecthefuture.org)

Carrara, S., Alves Dias, P., Plazzotta, B., & Pavel, C. (2020). Raw materials demand for wind and solar PV technologies in the transition towards a decarbonised energy system (EUR 30095 EN). Publications Office of the European Union. <https://doi.org/10.2760/160859>

California Department of Tax and Fee Administration. (n.d.). *Lithium extraction excise tax: Getting started* (conversion factors including $\text{Li}_2\text{O} \rightarrow \text{LCE} = 2.473$). Retrieved from <https://cdtfa.ca.gov/taxes-and-fees/lithium-extraction-excise-tax/getting-started.htm> [CDTFA](https://cdtfa.ca.gov)

Davis. (2021). Lithium-ion battery material circularity: Supplementary data (Tech. Rep.). https://escholarship.org/content/qt9cr072n9/qt9cr072n9_noSplash_120315e71bf54cab070b518b9187e83d.pdf

Dessemond, C., Lajoie-Leroux, F., Soucy, G., Laroche, N., & Ammar, S. (2019). Spodumene: The lithium market, resources and processes. *Minerals*, 9(6), 334. <https://doi.org/10.3390/min9060334> [MDPI](https://www.mdpi.com)

Denholm, P., Hand, M., Jackson, M., & Ong, S. (2009). Land-use requirements of modern wind power plants in the United States (NREL/TP-6A2-45834). National Renewable Energy Laboratory. <https://www.nrel.gov/docs/fy09osti/45834.pdf>

Dunn, J. (2022). Lithium-ion battery material circularity: Material availability, recycling economics, and the waste hierarchy (Doctoral dissertation). University of California, Davis. <https://escholarship.org/uc/item/7h92v5td>

Elshkaki, A., & Hilali, M. (2021). Raw materials demand for solar photovoltaics: Projections and implications. *Journal of Cleaner Production*, 305, 127248.

<https://doi.org/10.1016/j.jclepro.2021.127248>

Ellabban, O., & Alassi, A. (2021). Optimal hybrid microgrid sizing framework for the mining industry with three case studies from Australia. *IET Renewable Power Generation*, 15(4), 409–423.

<https://doi.org/10.1049/rpg2.12038>

Entwistle, J. A., Hursthouse, A. S., Reis, P. A. M., & Stewart, A. G. (2019). Metalliferous mine dust: Human health impacts and the potential determinants of disease in mining communities. *Current Pollution Reports*, 5(3), 67–83. <https://doi.org/10.1007/s40726-019-00108-5>

Feldman, D., Margolis, R., Denholm, P., & Stekli, J. (2016). *Exploring the potential competitiveness of utility-scale photovoltaics plus batteries with concentrating solar power, 2015–2030* (NREL/TP-6A20-66592). National Renewable Energy Laboratory. <https://www.nrel.gov/docs/fy16osti/66592.pdf>

Fthenakis, V. M., & Kim, H. C. (2009). Land use and electricity energy payback of CdTe photovoltaic systems. *Progress in Photovoltaics: Research and Applications*, 17(2), 88–98.

<https://doi.org/10.1002/pip.855>

Gazulla, M., Oliva, P., & Bobadilla, M. (2023). From emissions to resources: Mitigating the critical raw material supply chain vulnerability of renewable energy technologies. Retrieved from ResearchGate: https://www.researchgate.net/publication/378355748_From_emissions_to_resources_mitigating_the_critical_raw_material_supply_chain_vulnerability_of_renewable_energy_technologies

GlobalPetrolPrices.com. (n.d.). Global petrol and diesel prices. Retrieved July 10, 2025, from <https://www.globalpetrolprices.com/>

Góralczyk, M., Krot, P., Zimroz, R., & Ogonowski, S. (2020). Increasing energy efficiency and productivity of the comminution process in tumbling mills by indirect measurements of internal dynamics—An overview. *Energies*, 13(24), 6735. <https://doi.org/10.3390/en13246735> [MDPI](#)

Gunarathne, M. G. (n.d.). Final – ESGC Cost Performance Report 12-11-2020. Scribd. <https://www.scribd.com/document/562472138/Final-ESGC-Cost-Performance-Report-12-11-2020>

International Energy Agency (IEA), & Nuclear Energy Agency (NEA). (2020). *Projected costs of generating electricity 2020*. Paris, France: OECD Publishing. <https://doi.org/10.1787/a6002f3b-en>

International Renewable Energy Agency (IRENA). (2017). *Electricity storage and renewables: Costs and markets to 2030*. Retrieved from

https://www.climateaction.org/images/uploads/documents/IRENA_Electricity_Storage_Costs_2017.pdf

International Energy Agency. (2021). Net Zero by 2050: A roadmap for the global energy sector. IEA. <https://www.iea.org/reports/net-zero-by-2050>

International Energy Agency. (2022). Net Zero by 2050: A roadmap for the global energy sector. <https://www.iea.org/reports/net-zero-by-2050>

International Energy Agency Photovoltaic Power Systems Programme. (2020). Trends in Photovoltaic Applications: Survey report of selected IEA countries between 1992 and 2019 (Report IEA-PVPS T1-36:2020). https://iea-pvps.org/wp-content/uploads/2020/12/IEA_PVPS_Trends_2020.pdf

International Institute for Sustainable Development. (2024, August). Decarbonization of the mining sector: Scoping study on the role of mining in nationally determined contributions (IGF/Global). <https://www.iisd.org/system/files/2024-08/igf-decarbonization-mining-sector.pdf>

International Renewable Energy Agency. (2022). Power generation costs 2021. IRENA. https://www.irena.org/-/media/Files/IRENA/Agency/Publication/2022/Jul/IRENA_Power_Generation_Costs_2021.pdf

International Energy Agency. (2025). Electricity 2025. <https://www.iea.org/reports/electricity-2025>

Jessen, J. (2025, April 9). Top 10: Largest renewable energy projects. Energy Digital. Retrieved from <https://energydigital.com/top10/top-10-largest-renewable-energy-projects>

Luckeneder, S., Giljum, S., Schaffartzik, A., Maus, V., & Tost, M. (2021). Surge in global metal mining threatens vulnerable ecosystems. *Global Environmental Change*, 69, 102303. <https://doi.org/10.1016/j.gloenvcha.2021.102303>

Luderer, G., Pehl, M., Arvesen, A., Gibon, T., Bodirsky, B. L., de Boer, H. S., ... Hertwich, E. G. (2019). Environmental co-benefits and adverse side-effects of alternative power sector decarbonization strategies. *Nature Communications*, 10(1), 5229. <https://doi.org/10.1038/s41467-019-13067-8>

Nkambule, M. S., Hasan, A. N., & Shongwe, T. (2023). Performance and techno-economic analysis of optimal hybrid renewable energy systems for the mining industry in South Africa. *Sustainability*, 15(24), 16766. <https://doi.org/10.3390/su152416766>

Peiseler, L., Schenker, V., Schatzmann, K., Pfister, S., Wood, V., & Schmidt, T. (2024). Carbon footprint distributions of lithium-ion batteries and their materials. *Nature Communications*, 15, Article 10301. <https://doi.org/10.1038/s41467-024-54634-y>

- PetroP. (2020, January 22). Solar panels and wind turbine [Photograph]. DepositPhotos.
<https://depositphotos.com/photo/solar-panels-and-wind-turbine-334720368.html>
- Pouresmaieli, M., & Ataei, M. (2023). Integration of renewable energy and sustainable development with strategic planning in the mining industry. *Results in Engineering*, 20, Article 101412.
<https://doi.org/10.1016/j.rineng.2023.101412>
- Rasafi, T. E., Nouri, M., & Haddioui, A. (2017). Metals in mine wastes: Environmental pollution and soil remediation approaches – A review. *Geosystem Engineering*, 24(3), 157–172.
<https://doi.org/10.1080/12269328.2017.1400474>
- Samatar, A. M., Lekbir, A., Mekhilef, S., Mokhlis, H., Tey, K. S., & Alassaf, A. (2025). Techno-economic and environmental analysis of a fully renewable hybrid energy system for sustainable power infrastructure advancement. *Scientific Reports*, 15, Article 12140. <https://doi.org/10.1038/s41598-025-96401-z>
- Smith, K., Shi, Y., Wood, E., & Pesaran, A. (2017). Life prediction model for grid-connected Li-ion battery energy storage system: Preprint. National Renewable Energy Laboratory. Retrieved from <https://docs.nrel.gov/docs/fy17osti/67102.pdf>
- S&P Global. (2024, December 24). Mine Economics [Data set]. S&P Global.
- Stylos, N., & Koroneos, C. (2014). Life cycle assessment of photovoltaic modules. *Renewable Energy*, 66, 448–456. [Exergetic life cycle assessment of a grid-connected, polycrystalline silicon photovoltaic system | The International Journal of Life Cycle Assessment](#)
- Thomson, R. C., & Harrison, G. P. (2015). Life cycle costs and carbon emissions of wind power: Executive summary. ClimateXChange. Retrieved from http://www.climateexchange.org.uk/index.php/download_file/557/338/
- Tong, D., Farnham, D. J., Duan, L., Zhang, Q., Lewis, N. S., Caldeira, K., & Davis, S. J. (2021). Geophysical constraints on the reliability of solar and wind power worldwide. *Nature Communications*, 12, Article 6146. <https://doi.org/10.1038/s41467-021-26355-z>
- Torres, D., Pérez, K., Galleguillos Madrid, F. M., Leiva, W. H., Gálvez, E., Salinas-Rodríguez, E., Gallegos, S., Jamett, I., Castillo, J., Saldana, M., & Toro, N. (2024). Salar de Atacama lithium and potassium productive process. *Metals*, 14(10), 1095. <https://doi.org/10.3390/met14101095>

World Bank. (2020, April). Commodity markets outlook: April 2020.

<https://documents1.worldbank.org/curated/en/543311587659880031/pdf/Commodity-Markets-Outlook-April-2020.pdf>

Wang, Z., Wang, Y., Ding, Q., Wang, C., & Zhang, K. (2020). *Energy storage economic analysis of multi-application scenarios in an electricity market: A case study of China*. Sustainability, 12(20), 8703. <https://doi.org/10.3390/su12208703>

Appendices

Appendix A. Annual energy demand and energy source of mining sites

Table A1. Annual energy demand of each site

| Mining site | Source of Energy | Energy demand (GWh) |
|-------------|------------------|---------------------|
| Site 1 | Diesel | 73,64626484 |
| Site 2 | Diesel | 3,897244297 |
| Site 3 | Diesel | 138,689733 |
| Site 4 | Diesel | 242,7799443 |
| Site 5 | Diesel | 231,4273161 |
| Site 6 | Diesel | 494,1526596 |
| Site 7 | Grid | 64,6 |
| Site 8 | Diesel | 298,4251407 |
| Site 9 | Diesel | 687,1662665 |
| Site 10 | Diesel | 164,2579507 |
| Site 11 | Diesel | 314,1978469 |
| Site 12 | Diesel | 8,795077382 |
| Site 13 | Diesel | 502,0997697 |
| Site 14 | Diesel | 293,2364415 |

| | | |
|----------------|--------|-------------|
| Site 15 | Diesel | 1013,006237 |
| Site 16 | Diesel | 454,8798483 |
| Site 17 | Grid | 5,603116883 |
| Site 18 | Grid | 141,38045 |
| Site 19 | Diesel | 43,82395645 |
| Site 20 | Grid | 23,8719 |
| Site 21 | Grid | 121,6851833 |
| Site 22 | Grid | 272,8441875 |
| Site 23 | Grid | 31,73583333 |
| Site 24 | Grid | 2,747168831 |
| Site 25 | Diesel | 220,2679408 |
| Site 26 | Diesel | 224,7733624 |
| Site 27 | Diesel | 628,0043081 |
| Site 28 | Grid | 120,9823333 |
| Site 29 | Diesel | 92,96514149 |
| Site 30 | Grid | 150,3402338 |
| Site 31 | Grid | 105,1120779 |
| Site 32 | Grid | 179,9357273 |
| Site 33 | Grid | 176,772961 |
| Site 34 | Grid | 136,3210067 |
| Site 35 | Grid | 20,46231325 |
| Site 36 | Grid | 353,5742267 |
| Site 37 | Grid | 1063,053891 |
| Site 38 | Grid | 194,6842188 |
| Site 39 | Grid | 384,5554844 |

Appendix B. Techno-economic assessment inputs

Table B1. Parameters (inputs) for techno-economic assessment

| Parameter | Value | Unit |
|-----------|-------|------|
|-----------|-------|------|

| | | |
|-------------------------|------|--------|
| PV cost | 758 | \$/kW |
| PV O&M rate | 1.5 | % |
| Wind cost | 1160 | \$/kW |
| Wind O&M | 3 | % |
| Battery cost | 273 | \$/kWh |
| Batt. O&M | 0.43 | % |
| Battery lifetime | 10 | years |
| Mine life | 20 | years |

Sources: IRENA (2022) [technology CAPEX/O&M]; Mongird et al. (2020) [battery O&M]; Author's assumptions[Battery and Mine lifetime].

Table B2. Discount rates by country group

| Country group | discount rate |
|-----------------|---------------|
| OECD | 5% |
| non-OECD | 7.5 % |

Sources: IRENA (2022).

Appendix C. Energy-supply assumption robustness

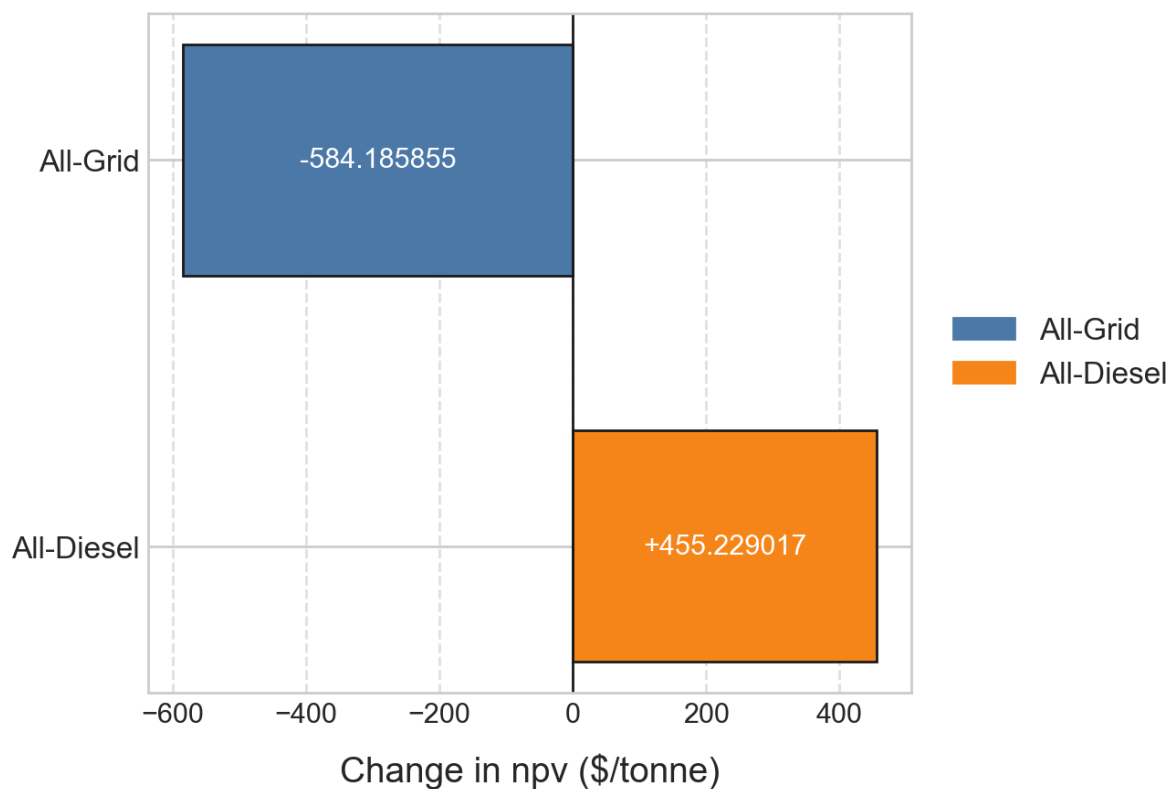


Figure C1. Change in IRR under energy supply scenario

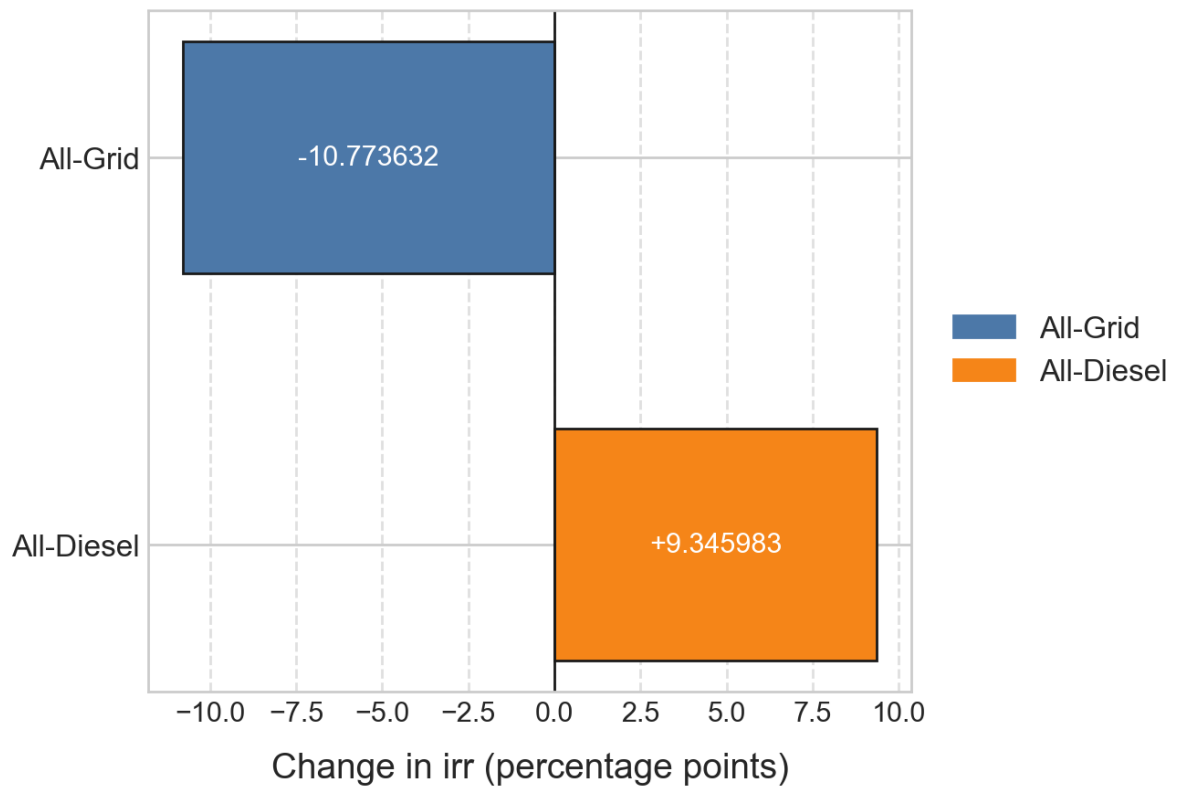


Figure C2. Change in mean Net present value per ton of LCE produced under energy supply scenario

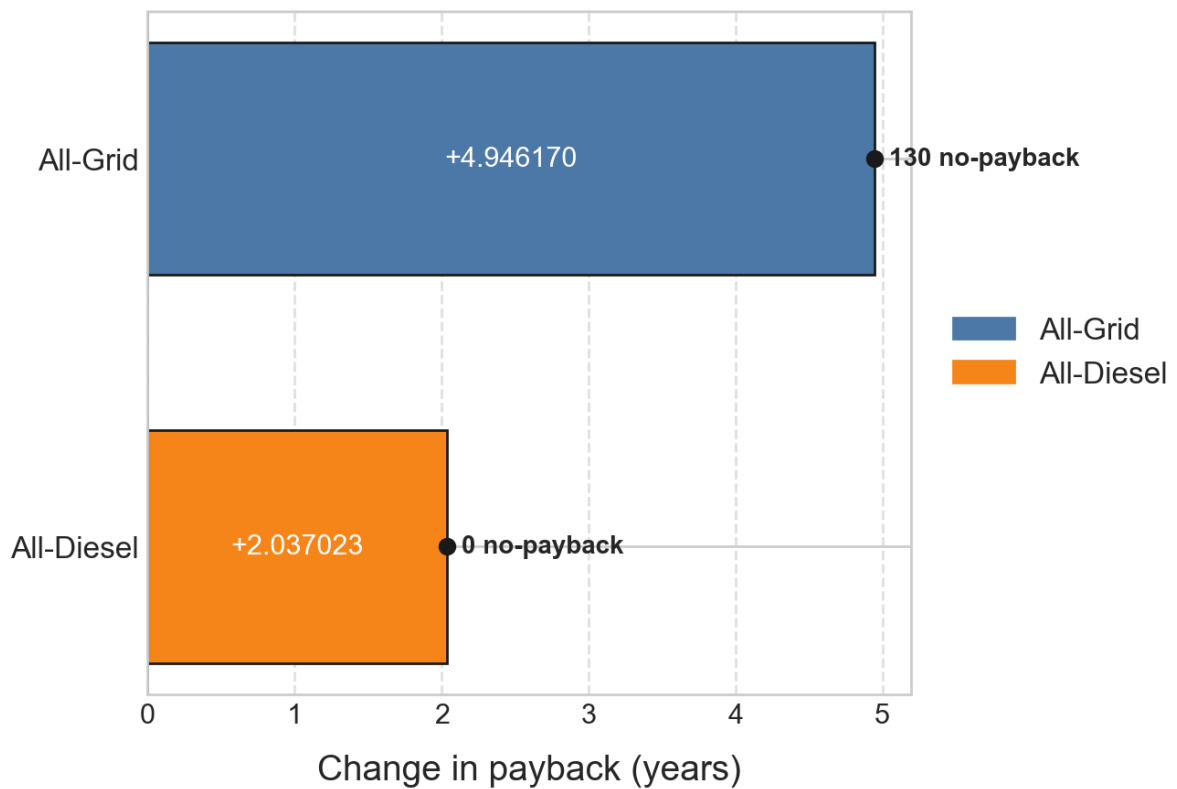


Figure C3. Change in mean payback period under energy supply scenario

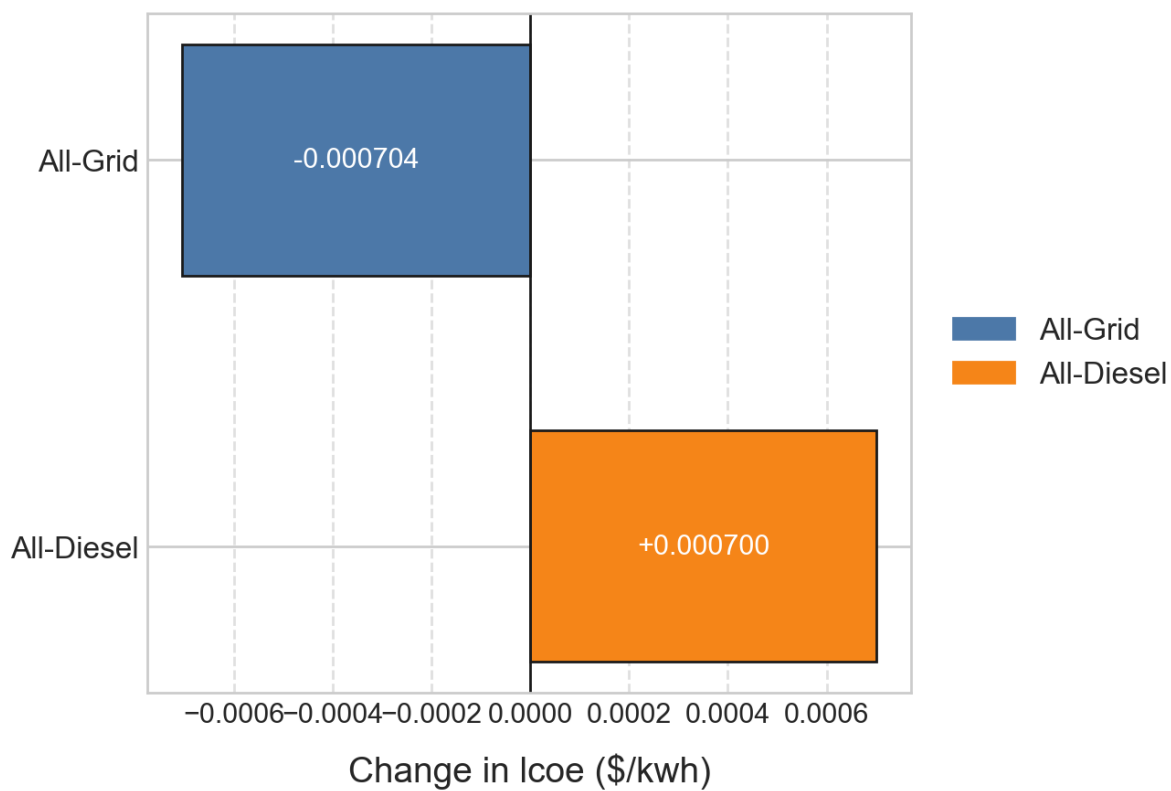


Figure C4. Change in mean levelized cost of energy under energy supply scenario

Appendix D. Mine life assumption robustness

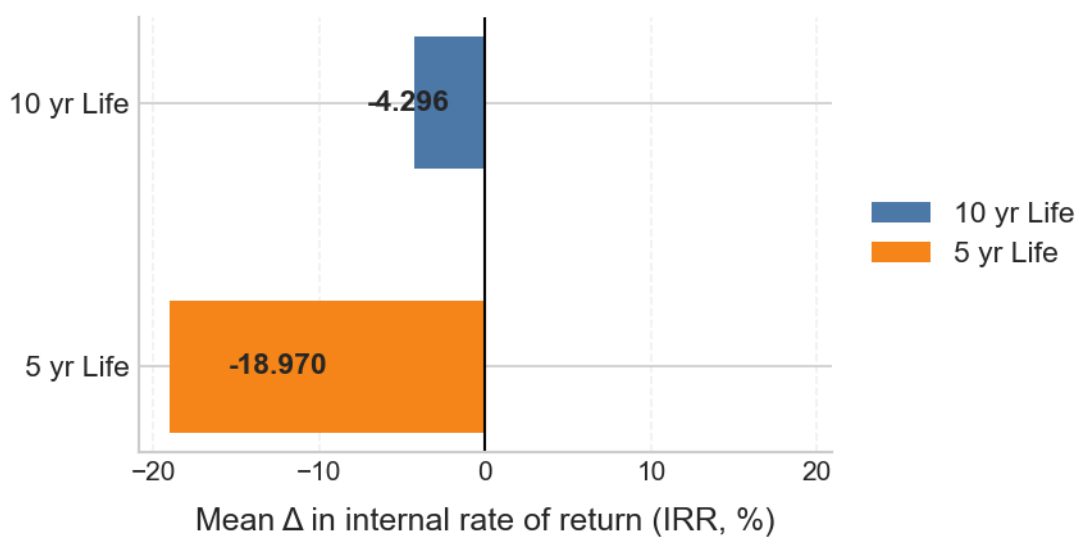


Figure D1. Impact of shortened mine life on internal rate of return

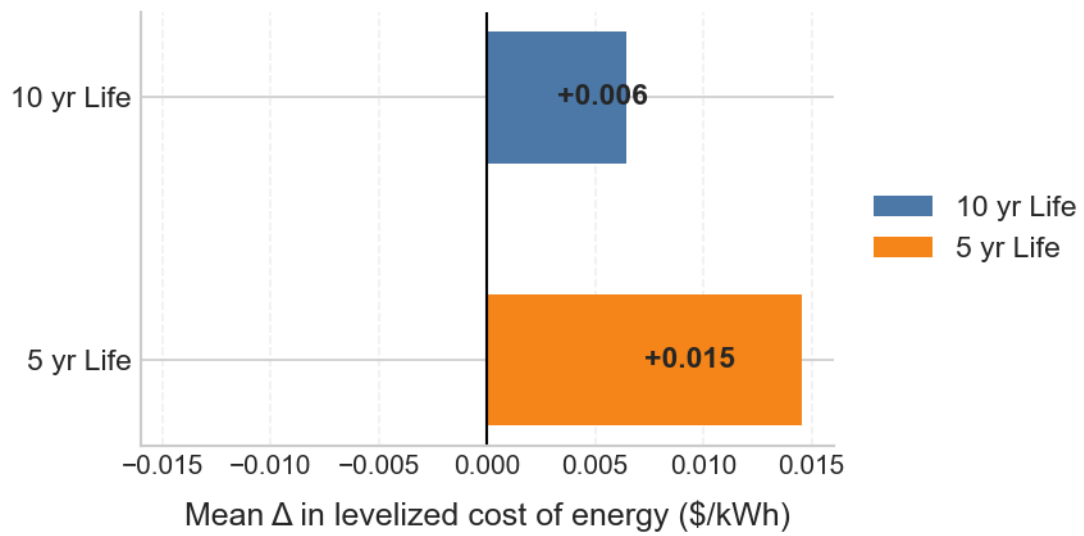


Figure D2. Impact of shortened mine life on levelized cost of energy

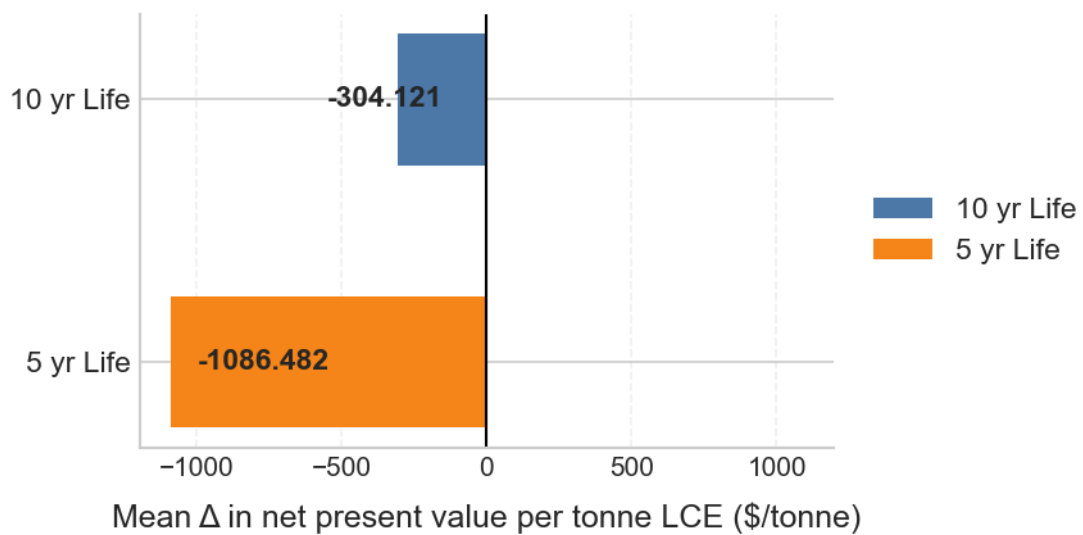


Figure D3. Impact of shortened mine life on mean net present value per tonne of LCE

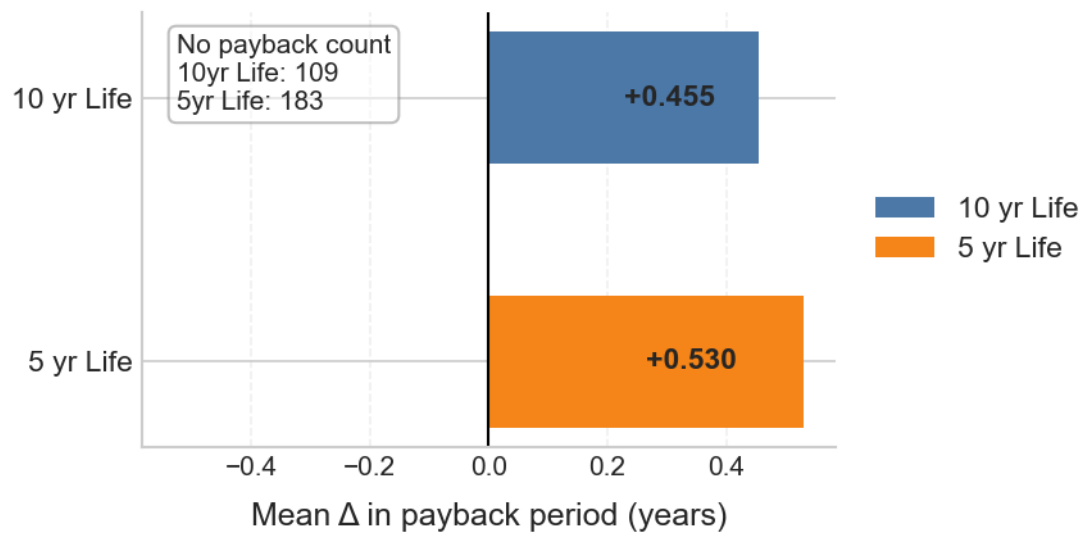


Figure D4. Impact of shortened mine life on mean payback period and total no paybacks

Appendix E. Life-cycle inventory data

Table E1. Material intensity for solar PV, wind turbines and lithium-ion batteries

| Material | Solar (t / kW) | Wind (t / kW) | Battery (kg / kWh) |
|---------------------------------|----------------|---------------|--------------------|
| Silver (Ag) | 0.00002 | - | - |
| Copper (BOS cabling & fittings) | 0.0046 | - | - |
| Aluminium | 0.0075 | 0.0014 | 3.528 |
| Copper | - | 0.0016 | 0.946 |
| Neodymium | - | 0.00043 | - |
| Dysprosium | - | 0.00007 | - |
| Graphite | - | = | 1.085 |
| Lithium | - | - | 0.095 |

Sources: Carrara et al. (2020); Elshkaki & Hilali (2021) [PV/wind]; Davis (2021); Dunn (2022) [batteries]

Table E2. Land transformation per megawatt of installed capacity for fixed-tilt PV, onshore wind and utility-scale battery storage

| Technology | Land transformation (ha / MW) |
|------------------------------------|-------------------------------|
| Fixed-tilt PV | 1.15 |
| Onshore wind (Total direct impact) | 1.0 ± 0.7 |
| Utility-scale BESS (Li-ion, UK) | 0.0202 |

Sources: IEA-PVPS (2020); Barbose et al. (2024) [PV]; Denholm et al. (2009); Arvesen & Hertwich (2012) [wind]; Abdul Latif Jameel (2023) [BESS].

Table E3. Life-cycle greenhouse gas emission ranges (g CO₂-eq /kWh) for renewables, battery manufacturing and baseline electricity

| Source / Technology | Min (g CO ₂ -eq /kWh) | Max (g CO ₂ -eq /kWh) |
|--------------------------------|----------------------------------|----------------------------------|
| Onshore wind | 3 | 45 |
| Solar PV | 12.3 | 58.8 |
| Battery manufacturing (Li-ion) | 54 000 | 69 000 |
| Grid electricity (baseline) | 506 | 837 |
| Diesel generation (baseline) | 710 | 930 |

Sources: Peiseler et al. (2024); Stylos & Koroneos (2014); Luderer et al. (2019); IEA (2025).

Appendix F. Model parameters and baseline assumption

| Parameter | Unit | Value | Citation |
|------------------------------------|--------|------------|--|
| PV CAPEX | \$/kW | 758 | IRENA, 2022 |
| PV O&M rate | % | 0.015 | IRENA, 2022 |
| Wind CAPEX | \$/kW | 1160 | IRENA, 2022 |
| Wind O&M rate | % | 0.03 | IRENA, 2022 |
| Battery CAPEX | \$/kWh | 273 | IRENA, 2022 |
| Battery O&M rate | % | 0.0043 | IRENA, 2022 |
| Battery lifetime | years | 10 | Assumption |
| PV lifetime | years | 20 | Assumption |
| Wind lifetime | years | 20 | Assumption |
| Mine lifetime | years | 20 | Assumption |
| Discount rate (OECD) | % | 5 | IRENA, 2022 |
| Discount rate (non- OECD) | % | 7.5 | IRENA, 2022 |
| Salvage value | — | 0 | Assumption |
| Inflation / Price Escalation | % | 0 | Assumption |
| Depth of Discharge | % | 80 | Augustine & Blair, 2021 |
| Round-trip Efficiency | % | 85 | Augustine & Blair, 2021 |
| Diesel generator efficiency | % | 40 | Assumption |
| Overbuild factor | × | 1.5 | Tong et al., 2021 |
| Battery storage durations | hours | 3 or 12 | Tong et al., 2021 |
| PV module size (small/large) | MW | 0.25 / 0.5 | Assumption (standard commercial sizes) |
| Wind turbine size (small/large) | MW | 0.5 / 2.5 | Assumption (standard commercial sizes) |
| Battery module size | kWh | 13.5 / 100 | Assumption (standard commercial sizes) |

| | | | |
|---|---------------------------|---|---|
| Electricity consumption – Brine | kWh/LCE | Depends on country | Li et al., 2024 (ACS ES&T) |
| Electricity consumption – Hard Rock | kWh/LCE | 7,718 | Author’s calculation (0.025 kWh/kg × 0.008 kg Li ₂ O) |
| Electricity consumption per site | kWh | Back-calculated for each site from electricity cost and LCE | S&P Global Market Intelligence, 2025 |
| Grid/diesel prices | \$/kWh | Country-specific | GlobalPetrolPrices.com |
| Solar capacity factor | % | Country/regional average | Tong et al., 2021 |
| Wind capacity factor | % | Country/regional average | Tong et al., 2021 |
| Material Intensity (PV, Wind, Battery) | kg/kW or kg/kWh | Varies by material (see Appendix E) | Carrara et al., 2020 |
| Land Transformation (PV, Wind, Battery) | ha/MW | Varies by technology (see Appendix E) | Fthenakis & Kim, 2009; IEA-PVPS, 2020; Denholm et al., 2009; Arvesen & Hertwich, 2012; Elshkaki & Hilali, 2021; IEA, 2022; Abdul Latif Jameel, 2023 |
| Lifecycle CO₂ Emissions (PV, Wind, Battery) | g CO ₂ -eq/kWh | 3–930 depending on technology | Peiseler et al., 2024; Stylos & Koroneos, 2014; Luderer et al., 2019 |

Appendix G. System sizing by site

Table G.1 Renewable and battery storage sizing

| Site | Battery storage GWh | Battery storage GWh | Wind capacity (GW) | Solar capacity (GW) | Hybrid (GW) |
|------|---------------------|---------------------|--------------------|---------------------|-------------|
| | | | | | |

| | (3 hours) | (12 hours) | | | |
|---------|--------------|---------------|------|------|------|
| Mine_1 | 0,06 | 0,22 | 0,07 | 0,11 | 0,09 |
| Mine_2 | 0 | 0,01 | 0 | 0 | 0 |
| Mine_3 | 0,1 | 0,42 | 0,13 | 0,21 | 0,17 |
| Mine_4 | 0,18 | 0,73 | 0,2 | 0,35 | 0,28 |
| Mine_5 | 0,17 | 0,7 | 0,21 | 0,35 | 0,28 |
| Mine_6 | 0,37 | 1,49 | 0,41 | 0,71 | 0,56 |
| Mine_7 | 0,05 | 0,2 | 0,06 | 0,1 | 0,08 |
| Mine_8 | 0,23 | 0,9 | 0,2 | 0,37 | 0,29 |
| Mine_9 | 0,52 | 2,08 | 0,47 | 0,84 | 0,65 |
| Mine_10 | 0,12 | 0,5 | 0,14 | 0,23 | 0,19 |
| Mine_11 | 0,24 | 0,95 | 0,16 | 0,32 | 0,24 |
| Mine_12 | 0,01 | 0,03 | 0,01 | 0,01 | 0,01 |
| Mine_13 | 0,38 | 1,52 | 0,38 | 0,72 | 0,55 |
| Mine_14 | 0,22 | 0,89 | 0,2 | 0,36 | 0,28 |
| Mine_15 | 0,77 | 3,06 | 0,69 | 1,24 | 0,96 |
| Mine_16 | 0,34 | 1,37 | 0,31 | 0,56 | 0,43 |
| Mine_17 | 0 | 0,02 | 0,01 | 0,01 | 0,01 |
| Mine_18 | 0,11 | 0,43 | 0,08 | 0,18 | 0,13 |
| Mine_19 | 0,03 | 0,13 | 0,04 | 0,07 | 0,05 |
| Mine_20 | 0,02 | 0,07 | 0,02 | 0,03 | 0,02 |
| Mine_21 | 0,09 | 0,37 | 0,07 | 0,16 | 0,11 |
| Mine_22 | 0,21 | 0,82 | 0,16 | 0,5 | 0,33 |
| Mine_23 | 0,02 | 0,1 | 0,02 | 0,04 | 0,03 |
| Mine_24 | 0 | 0,01 | 0 | 0 | 0 |
| Mine_25 | 0,17 | 0,67 | 0,15 | 0,27 | 0,21 |
| Mine_26 | 0,17 | 0,68 | 0,15 | 0,27 | 0,21 |
| Mine_27 | 0,47 | 1,9 | 0,56 | 0,95 | 0,75 |
| Mine_28 | 0,09 | 0,37 | 0,07 | 0,16 | 0,11 |
| Mine_29 | 0,07 | 0,28 | 0,08 | 0,14 | 0,11 |

| | | | | | |
|---------|------|------|------|------|------|
| Mine_30 | 0,11 | 0,45 | 0,14 | 0,23 | 0,18 |
| Mine_31 | 0,08 | 0,32 | 0,1 | 0,16 | 0,13 |
| Mine_32 | 0,14 | 0,54 | 0,16 | 0,27 | 0,22 |
| Mine_33 | 0,13 | 0,53 | 0,16 | 0,27 | 0,21 |
| Mine_34 | 0,1 | 0,41 | 0,09 | 0,17 | 0,13 |
| Mine_35 | 0,02 | 0,06 | 0,02 | 0,02 | 0,02 |
| Mine_36 | 0,27 | 1,07 | 0,24 | 0,43 | 0,34 |
| Mine_37 | 0,8 | 3,21 | 0,78 | 1,14 | 0,96 |
| Mine_38 | 0,15 | 0,59 | 0,15 | 0,21 | 0,18 |
| Mine_39 | 0,29 | 1,16 | 0,28 | 0,41 | 0,35 |

Appendix H. Material intensity results

Table H.1 Per Technology material intensity per 1000 t LCE (medians)

| Technology | Aluminium | Copper | Graphite | Silver | Neodymium | Dysprosium | Lithium |
|------------|-----------|--------|----------|--------|-----------|------------|---------|
| Solar | 130.91 | 66.60 | 13.47 | 0.21 | 0.00 | 0.00 | 1.18 |
| Wind | 55.85 | 22.86 | 13.47 | 0.00 | 2.53 | 0.41 | 1.18 |
| Hybrid | 71.79 | 27.87 | 13.47 | 0.05 | 0.63 | 0.10 | 1.18 |

Table H.2 Per technology material intensity per GWh delivered annually (medians)

| Technology | Aluminium | Copper | Graphite | Silver | Neodymium | Dysprosium | Lithium |
|------------|-----------|--------|----------|--------|-----------|------------|---------|
| Solar | 0.8698 | 0.3833 | 0.1028 | 0.0013 | 0.0000 | 0.0000 | 0.0090 |
| Wind | 0.3911 | 0.1550 | 0.1028 | 0.0000 | 0.0158 | 0.0025 | 0.0090 |
| Hybrid | 0.4768 | 0.1824 | 0.1028 | 0.0003 | 0.0040 | 0.0006 | 0.0090 |

Table H.3 Per country material intensity per 1000 t LCE (medians)

| Country | Aluminium | Copper | Graphite | Silver | Neodymium | Dysprosium | Lithium |
|---------------|-----------|--------|----------|--------|-----------|------------|---------|
| Argentina | 70.24 | 23.71 | 10.23 | 0.04 | 0.35 | 0.06 | 0.90 |
| Australia | 75.02 | 33.89 | 11.38 | 0.05 | 0.63 | 0.10 | 1.00 |
| Brazil | 64.64 | 25.28 | 11.79 | 0.03 | 0.45 | 0.07 | 1.03 |
| Canada | 113.05 | 39.40 | 17.98 | 0.08 | 0.54 | 0.09 | 1.57 |
| Chile | 75.24 | 28.21 | 14.15 | 0.03 | 0.51 | 0.08 | 1.24 |
| China | 134.02 | 48.48 | 14.48 | 0.08 | 1.04 | 0.17 | 1.27 |
| Mali | 219.46 | 77.61 | 35.85 | 0.12 | 1.42 | 0.23 | 3.14 |
| Portugal | 164.36 | 61.15 | 25.81 | 0.09 | 1.54 | 0.25 | 2.26 |
| United States | 57.92 | 21.96 | 10.77 | 0.03 | 0.41 | 0.07 | 0.94 |
| Zimbabwe | 72.99 | 32.59 | 10.25 | 0.06 | 0.74 | 0.12 | 0.90 |

Table H.4 Per country material intensity per GWh delivered annually (medians)

| Country | Aluminium | Copper | Graphite | Silver | Neodymium | Dysprosium | Lithium |
|---------------|-----------|--------|----------|--------|-----------|------------|---------|
| Argentina | 0.5962 | 0.2103 | 0.1026 | 0.0003 | 0.0029 | 0.0004 | 0.0090 |
| Australia | 0.5864 | 0.2122 | 0.1024 | 0.0003 | 0.0036 | 0.0005 | 0.0090 |
| Brazil | 0.5447 | 0.2123 | 0.1028 | 0.0003 | 0.0029 | 0.0004 | 0.0089 |
| Canada | 0.6443 | 0.2245 | 0.1024 | 0.0004 | 0.0031 | 0.0004 | 0.0090 |
| Chile | 0.5595 | 0.2108 | 0.1024 | 0.0003 | 0.0040 | 0.0004 | 0.0089 |
| China | 0.6438 | 0.2319 | 0.1025 | 0.0004 | 0.0048 | 0.0004 | 0.0089 |
| Mali | 0.6272 | 0.2218 | 0.1024 | 0.0003 | 0.0040 | 0.0003 | 0.0090 |
| Portugal | 0.6541 | 0.2434 | 0.1027 | 0.0004 | 0.0061 | 0.0004 | 0.0089 |
| United States | 0.5519 | 0.2093 | 0.1026 | 0.0003 | 0.0040 | 0.0006 | 0.0090 |
| Zimbabwe | 0.6300 | 0.2257 | 0.1024 | 0.0003 | 0.0045 | 0.0008 | 0.0089 |

APPENDIX I. Hard rock mining sites energy intensity calculations

Electricity per kg Li_2O = $(0.025 \text{ kWh/kg material}) \div (0.008 \text{ kg Li}_2\text{O/kg material}) = 3.125 \text{ kWh/kg Li}_2\text{O}$
(Burgess, 2012; Góralczyk, Krot, Zimroz, & Ogonowski, 2020; Dessemond, Lajoie-Leroux, Soucy, Laroche, & Ammar, 2019).

Electricity per kg LCE = $(3.125 \text{ kWh/kg Li}_2\text{O}) \times (2.473 \text{ kg LCE/kg Li}_2\text{O}) = 7.71875 \text{ kWh/kg LCE}$
(California Department of Tax and Fee Administration [CDTFA], n.d.).

Electricity per tonne LCE = 7,718.75 kWh/t LCE

APPENDIX K. Diesel scenarios, energy demand (kwh/LCE)

Effective diesel electricity price (USD/kWh):

$$C_{\text{diesel}} = (\$/L) / (0.846 \text{ kg/L} * 11.83 \text{ kWh/kg} * \eta)$$

4) where η = diesel generator efficiency (0.35)

5) $\$/L$ = diesel price

Electricity per tonne LCE (kWh/t LCE):

$$\text{Electricity intensity (kWh/LCE)} = (\text{Electricity spend per LCE } [$/t]) / c_{\text{diesel}}$$